INSTITUTE OF PHYSICS PUBLISHING JOURNAL OF PHYSICS B: ATOMIC, MOLECULAR AND OPTICAL PHYSICS

J. Phys. B: At. Mol. Opt. Phys. **39** (2006) 243–269 doi:10.1088/0953-4075/39/2/004

Benchmark Kantorovich calculations for three particles on a line

O Chuluunbaatar[1], A A Gusev[1], M S Kaschiev[2], V A Kaschieva[3], A Amaya-Tapia[4], S Y Larsen[5] and S I Vinitsky[1]

[1] Joint Institute for Nuclear Research, Dubna, Moscow region 141980, Russia
[2] Institute of Mathematics and Informatics, Sofia, Bulgaria
[3] Department of Mathematics, Technical University, Sofia, Bulgaria
[4] Centro de Ciencias Fisicas, UNAM, Cuernavaca, Morelos, Mexico
[5] Temple University, Philadelphia, USA

Received 29 June 2005, in final form 13 October 2005
Published 14 December 2005
Online at stacks.iop.org/JPhysB/39/243

Abstract

A Kantorovich approach is used to solve for the eigenvalue and the scattering properties associated with a multi-dimensional Schrödinger equation. It is developed within the framework of a conventional finite element representation of solutions over a hyperspherical coordinate space. Convergence and efficiency of the proposed schemes are demonstrated in the case of an exactly solvable 'benchmark' model of three identical particles on a line, with zero-range attractive pair potentials and below the three-body threshold. In this model all the 'effective' potentials, and 'coupling matrix elements', of the set of resulting close-coupling radial equations, are calculated using analytical formulae. Variational formulations are developed for both *the bound-state energy and the elastic scattering problem*. The corresponding numerical schemes are devised using a finite element method of high order accuracy.

1. Introduction

One of the most popular and widely used approaches for solving the quantum-mechanical three-body problem, with pair Coulomb and short-ranged interactions, is the adiabatic representation method [1–5]. In the framework of the hyperspherical coordinates formulation of this method [5–11], the hyperradius ρ is treated as a slowly varying adiabatic variable, analogous to the internuclear distance in the Born–Oppenheimer approximation for molecules [1]. From the mathematical point of view, this approach is well known as the Kantorovich method (KM). It enables the reduction of a boundary value problem for a multi-dimensional Schrödinger equation (MDSE), to a one-dimensional one, by using a set of solutions of an auxiliary parametric eigenvalue problem [12]. An essential part in the implementation of the KM is the computation of variable coefficients, so-called, *the effective potentials and coupling matrix elements* for the final system of the ordinary second-order differential equations [10].

These coefficients are the eigenvalues and integrals over surface eigenfunctions of the auxiliary eigenvalue problem and their derivatives with respect to the adiabatic variable. In real applications, an efficient and stable computation of derivatives of the adiabatic eigenfunctions and the corresponding integrals with the accuracy comparable with the one achieved for adiabatic eigenfunctions presents a serious challenge for most of the numerical approaches involved in various types of calculations within the adiabatic representation method. In order to eliminate derivatives of the adiabatic surface eigenfunctions in hyperradius, the sector adiabatic approach is widely used. The price for using this approximation is a slower convergence of the adiabatic basis and therefore a larger number of hyperradial equations to be solved in order to get the required accuracy of the S-matrix elements [11].

A new calculation method [13] for the matrix elements of the radial coupling potentials within the KM to the required accuracy, allows one to use them in both the bound states and scattering calculations of three-body problem with realistic potentials such as the pair Coulomb potentials. In the same work the benchmark calculations of *the ground-state energy of the helium atom and negative hydrogen ion* were performed. Efficiency of the KM has been shown recently [14] in high-accuracy calculations approximately 12 significant digits of low-lying excited states of a hydrogen atom in a strong magnetic field. Applications of the method to scattering problems should also be very useful and promising.

The main idea of this paper is to formulate the KM to solve the eigenvalue and scattering problems for MDSE. In this method, the multi-dimensional boundary problem is reduced to a system of second-order ordinary differential equations with variable coefficients on a semi-axis by means of expansion of the solution in a set of orthogonal solutions of an auxiliary parametric eigenvalue problem. A finite element method (FEM) is then applied to construct a stable numerical iteration scheme, yielding a solution of the corresponding boundary value problem (for the system of ordinary differential equations) with an arbitrary specification in the 'space' step. Note that the various versions of FEM have been applied successfully in calculations of molecular dynamics and electronic structure for bound states [15, 16] and scattering problems [17, 18]. However, the three-body scattering calculations with pair Coulomb potentials are rather complicate in the framework of the KM, because the variable coefficients in ordinary differential equations and in the corresponding solutions can have asymptotic behaviours which are long-ranged [10, 11]. That is why one has to be very careful in the formulation of the boundary problems under consideration.

As a benchmark, we consider, below, the known exactly soluble model of three identical particles on a line, with zero-range attractive pair potentials, below three-body threshold, discussed in [19–22]. In this model *all the effective potentials and coupling matrix elements, of a benchmark set of close-coupling radial equations, are evaluated explicitly*. We construct appropriate variational formulations [23] for both *the bound-state and the elastic scattering problems* in the framework of the KM, using Rayleigh–Ritz's and Hulthèn's variation functionals [24, 25]. The corresponding stable numerical schemes are realized using FEMs of high order accuracy [26–28]. We verify the accuracy of these schemes, and examine their rate of convergence to the known exact results, as a function of the number of basis functions.

This paper is organized as follows. In section 2 the KM is formulated for our 'benchmark' model—both for the multichannel eigenvalue and for the scattering problems in the infinite domain. All the needed matrix elements are determined here by explicit analytical formulae. The reformulation of both problems to involve a finite interval (i.e. not extending to infinity) is performed in section 3. All the asymptotic expressions needed to determine the solutions, and the unknown phase shift, from the variational iteration schemes, are presented. The high-order approximations by the finite element method are formulated in section 4. In section 5, the

numerical results obtained in the framework of the FEMs are discussed. In conclusion, we look at the perspectives for further applications of this approach.

2. Statement of the problem

We consider three identical particles in the centre-of-mass reference frame (CMRF) described by the Jacobi coordinates,

$$\eta = \sqrt{\frac{1}{2}}(x_1 - x_2), \qquad \xi = \sqrt{\frac{2}{3}}\left(\frac{x_1 + x_2}{2} - x_3\right),$$

in the plane $\mathbf{R}^2$, where $\{\{x_1, x_2, x_3\} \in \mathbf{R}^3 | x_1 + x_2 + x_3 = 0\}$ are the Cartesian coordinates of the particles on a line. In polar coordinates

$$\eta = \rho\cos\theta, \qquad \xi = \rho\sin\theta, \qquad -\frac{\pi}{6} < \theta \leqslant 2\pi - \frac{\pi}{6}, \qquad 0 \leqslant \rho < \infty,$$

the Schrödinger equation for the wavefunction $\Psi(\rho, \theta)$ takes the form

$$-\left[\frac{1}{\rho}\frac{\partial}{\partial\rho}\rho\frac{\partial}{\partial\rho} + \frac{1}{\rho^2}\frac{\partial^2}{\partial\theta^2}\right]\Psi(\rho,\theta) + V(\rho,\theta)\Psi(\rho,\theta) = 2E\Psi(\rho,\theta), \tag{1}$$

where E is the relative energy in the CMRF. To obtain an exact solution which can be used below for a comparison with the numerical results, we involve the sum of delta-functions for describing the pair interactions with identical finite strengths. Thus, $V(\rho, \theta)$ assumes the form

$$V(\rho,\theta) = 2g\sum_{n=-1}^{1}\delta\left(\sqrt{2}\rho\left|\cos\left(\theta - \frac{2\pi}{3}n\right)\right|\right), \tag{2}$$

where $g = \sqrt{2}c\bar{\kappa}$, and $\bar{\kappa} = \pi/6$ is the effective strength of the pair potential [19, 20, 22]. Further, we consider only the case of attraction ($c = -1$). In this case we have the bound pair state $\phi_0(\eta) = \sqrt{\bar{\kappa}}\exp(-\bar{\kappa}|\eta|)$ with the energy $-\epsilon_0^{(0)} = \bar{\kappa}^2$, so that $2E = q^2 + \epsilon_0^{(0)}$, where q is proportional to the relative momentum of the third particle with respect to the bound pair [20, 22].

Using a six-fold symmetric representation compatible with (2), we formulate the following boundary problem corresponding to equation (1) in the case $E < 0$ [22]:

$$-\left[\frac{1}{\rho}\frac{\partial}{\partial\rho}\rho\frac{\partial}{\partial\rho} + \frac{1}{\rho^2}\frac{\partial^2}{\partial\theta^2}\right]\Psi(\rho,\theta) = 2E\Psi(\rho,\theta), \tag{3}$$

with boundary conditions ($\theta_n \leqslant \theta < \theta_{n+1}$)

$$\begin{aligned} &\frac{1}{\rho}\frac{\partial\Psi(\rho,\theta_i)}{\partial\theta} = (-1)^{i-n}c\bar{\kappa}\Psi(\rho,\theta_i), \qquad i = n, n+1, \\ &\Psi(\rho,\theta_{n+1} - 0) = \Psi(\rho,\theta_{n+1} + 0), \end{aligned} \tag{4}$$

where $\theta_n = \bar{\kappa}(2n-1)$, $n = 0$–5, and we need to satisfy additional radial boundary conditions:

$$\begin{aligned} &\lim_{\rho\to 0}\rho\frac{\partial\Psi(\rho,\theta)}{\partial\rho} = 0, \\ &\Psi(\rho,\theta)|_{\rho\to\infty} \to \chi_0^{\mathrm{as}}(\rho)B_0^{\mathrm{as}}(\rho;\theta) + F(k,\theta)\sqrt{\frac{\pi}{2k\rho}}\exp(-k\rho). \end{aligned} \tag{5}$$

Here $B_0^{\mathrm{as}}(\rho;\theta)$ is the asymptotic surface function corresponding to $\phi_0(\eta)$ at large ρ (see appendix A), $F(k,\theta)$ is a function of $k = \sqrt{-2E} > 0$ and the function $\chi_0^{\mathrm{as}}(\rho)$ satisfies the following asymptotic conditions.

For the bound state with $2E \leqslant \epsilon_0^{(0)} = -\pi^2/36$, at $\bar{q}\rho \gg 1$

$$\chi_0^{\rm as}(\rho) = C\frac{\exp(-\bar{q}\rho)}{\sqrt{\rho}}(1 + O(\rho^{-1})), \tag{6}$$

where $\varepsilon = \bar{q}^2 = -q^2 = -2E + \epsilon_0^{(0)} \geqslant 0$ is the (unknown) binding energy of the three-body system and C is an unknown constant.

For the elastic scattering problem in the open channel $2E(q) > \epsilon_0^{(0)}$, i.e. for $0 < q < \bar{\kappa}$, at $q\rho \gg 1$

$$\chi_0^{\rm as}(\rho) = \frac{\sin(q\rho + \delta)}{\sqrt{q\rho}} + O(\rho^{-3/2}), \tag{7}$$

where $\delta = \delta(q)$ is the (unknown) phase shift.

For our model (2), equation (1) can be solved exactly, yielding the energy $-2E_b^{\rm exact} = 4\bar{\kappa}^2$ for the unique bound state, $-2E_{hb}^{\rm exact} = \bar{\kappa}^2$ for a half-bound state (or zero-energy resonance), and a phase shift equal to:

$$\delta^{\rm exact}(q) = \frac{3\pi}{2} - \arctan\left(\frac{4\bar{\kappa}q}{\sqrt{3}(\bar{\kappa}^2 - q^2)}\right) \tag{8}$$

for the elastic scattering problem for $0 < q < \bar{\kappa}$. It also gives an infinite elastic scattering length: $a_0 = -\lim\limits_{q\to 0}(\tan(\delta)/q) = -\infty$ [20].

2.1. The Kantorovich method

Consider a formal expansion of the solution of equations (1), (2) using the infinite set of one-dimensional basis functions $B_j(\rho;\theta) \in W_2^1(-\pi/6, 2\pi - \pi/6)$:

$$\Psi(\rho,\theta) = \sum_{j=0}^{N-1} \chi_j(\rho) B_j(\rho;\theta). \tag{9}$$

In equation (9), the functions $\boldsymbol{\chi}(\rho) = (\chi_0(\rho), \ldots, \chi_{N-1}(\rho))^T$ are unknown, and the surface functions $\boldsymbol{B}(\rho;\theta) = (B_0(\rho;\theta), \ldots, B_{N-1}(\rho;\theta))^T$ form an orthonormal basis with respect to the independent angular variable $-\pi/6 < \theta \leqslant 2\pi - \pi/6$ for each value of ρ which is treated here as a given parameter. In the Kantorovich approach [12], the functions $B_j(\rho;\theta)$ are determined as solutions of the following one-dimensional parametric eigenvalue problem:

$$\begin{aligned}
&-\frac{1}{\rho^2}\frac{\partial^2 B_j(\rho;\theta)}{\partial\theta^2} = \epsilon_j(\rho) B_j(\rho;\theta), \qquad \theta_n \leqslant \theta < \theta_{n+1}, \qquad n = 0\text{–}5,\\
&\frac{1}{\rho}\frac{\partial B_j(\rho;\theta_i)}{\partial\theta} = (-1)^{i-n} c\bar{\kappa} B_j(\rho;\theta_i), \qquad i = n, n+1,\\
&B_j(\rho;\theta_{n+1} - 0) = B_j(\rho;\theta_{n+1} + 0).
\end{aligned} \tag{10}$$

The eigenfunctions of this problem are normalized as follows:

$$\langle B_i(\rho;\theta) \mid B_j(\rho;\theta)\rangle = \sum_{n=0}^{5}\int_{\theta_n}^{\theta_{n+1}} B_i^*(\rho;\theta) B_j(\rho;\theta)\,{\rm d}\theta = \delta_{ij}. \tag{11}$$

After using expansion (9) in the Rayleigh–Ritz variational functional (see [13]) and minimizing the functional, the solution of equations (1), (2) reduces to a solution of the finite set of N ordinary second-order differential equations. This leads to the determination of the energy E, in the eigenvalue problem, and the coefficients $\boldsymbol{\chi} \equiv \boldsymbol{\chi}(\rho)$ of expansion (9)

$$(H - 2E)\boldsymbol{\chi} \equiv -\mathbf{I}\frac{1}{\rho}\frac{\rm d}{{\rm d}\rho}\rho\frac{{\rm d}\boldsymbol{\chi}}{{\rm d}\rho} + \mathbf{V}\boldsymbol{\chi} + \mathbf{Q}\frac{{\rm d}\boldsymbol{\chi}}{{\rm d}\rho} + \frac{1}{\rho}\frac{{\rm d}\rho\mathbf{Q}\boldsymbol{\chi}}{{\rm d}\rho} - 2E\mathbf{I}\boldsymbol{\chi} = 0, \qquad \lim_{\rho\to 0}\rho\frac{{\rm d}\boldsymbol{\chi}}{{\rm d}\rho} = 0. \tag{12}$$

The boundary conditions at $\rho \to \infty$ are given by (6) or (7) depending on the problem. In these expressions the matrix $\mathbf{V}$ is symmetric and $\mathbf{Q}$ is skew-symmetric. They are given by

$$\begin{aligned} V_{ij}(\rho) &= H_{ij}(\rho) + 0.5(\epsilon_i(\rho) + \epsilon_j(\rho))\delta_{ij}, \\ H_{ij}(\rho) &= \left\langle \frac{\partial}{\partial\rho} B_i(\rho;\theta) \,\middle|\, \frac{\partial}{\partial\rho} B_j(\rho;\theta) \right\rangle, \\ Q_{ij}(\rho) &= -Q_{ji}(\rho) = -\left\langle B_i(\rho;\theta) \,\middle|\, \frac{\partial}{\partial\rho} B_j(\rho;\theta) \right\rangle. \end{aligned} \tag{13}$$

In this paper, it suffices for us to consider only a part of the total adiabatic (surface) basis. It is totally symmetric, of course, and—in the Schrödinger equation—'links', through the 'coupling' matrix elements, only to itself. It allows us to discuss the bound state and the resonance, and the 2 + 1 scattering below threshold (i.e. in both cases, involving the 'lowest' states of the system). An additional part of the basis involves 'sine'-type Bs—in contrast to the 'cosine'-type displayed below. It also 'links' amplitudes, of the solution of the Schrödinger equation, associated only with its basis elements.

A way to understand this behaviour is to realize that each B reduces to a harmonic when ρ tends to zero, and that, since the interaction is symmetric, the B adopts the symmetry of the harmonic. The harmonics are classified as to their permutation properties in [8]. The 'cosine' Bs are associated with 'cosine'-type harmonics involving the orders 0 mod 3 and even. The 'sine'-type harmonics involve the orders 0 mod 3 and odd. Note that the explicit analytical expressions for the 'sine'-type harmonics and corresponding transcendental equations are given in [22].

As is shown in paper [19], the boundary problem (10), (11) then has, for our purposes, the analytical solutions

$$\begin{aligned} B_0(\rho;\theta) &= \sqrt{\frac{y_0^2 - x^2}{\pi\left(y_0^2 - x^2\right) + |x|}} \cosh\left[6y_0\left(\theta - \frac{n\pi}{3}\right)\right], \\ B_j(\rho;\theta) &= \sqrt{\frac{y_j^2 + x^2}{\pi\left(y_j^2 + x^2\right) - |x|}} \cos\left[6y_j\left(\theta - \frac{n\pi}{3}\right)\right], \\ \epsilon_0(\rho) &= -\left(\frac{6y_0(\rho)}{\rho}\right)^2, \qquad \epsilon_j(\rho) = \left(\frac{6y_j(\rho)}{\rho}\right)^2, \end{aligned} \tag{14}$$

where n is an integer determined by $|\theta - n\pi/3| < \pi/6$, $n = 0$–5. The transcendental equations

$$\begin{aligned} &y_0(\rho)\tanh(\pi y_0(\rho)) = -x, \qquad 0 \leqslant y_0(\rho) < \infty, \qquad x = c\frac{\pi}{36}\rho, \\ &y_j(\rho)\tan(\pi y_j(\rho)) = x, \qquad j - \frac{1}{2} < y_j(\rho) < j, \qquad j = 1, 2, \ldots, \end{aligned} \tag{15}$$

follow from (10), (11). The functions $\epsilon_j(\rho)$ are determined by the roots $y_j(\rho)$ of these equations that are solved numerically (see, for example, figure 1).

Using the analytical expressions for the functions $B_j(\rho;\theta)$, $\epsilon_j(\rho)$, we find the matrix elements $H_{ij}(\rho)$ and $Q_{ij}(\rho)$ using the roots $y_j(\rho)$ and the parameter x:

$$\begin{aligned} Q_{0j}(\rho) &= -Q_{j0}(\rho) = -\frac{c\pi}{18}\frac{(-1)^j y_0 y_j}{\left(y_0^2 + y_j^2\right)\tilde{y}_0\tilde{y}_j}, \\ Q_{ij}(\rho) &= -Q_{ji}(\rho) = \frac{c\pi}{18}\frac{(-1)^{i+j} y_i y_j}{\left(y_i^2 - y_j^2\right)\tilde{y}_i\tilde{y}_j}, \end{aligned}$$

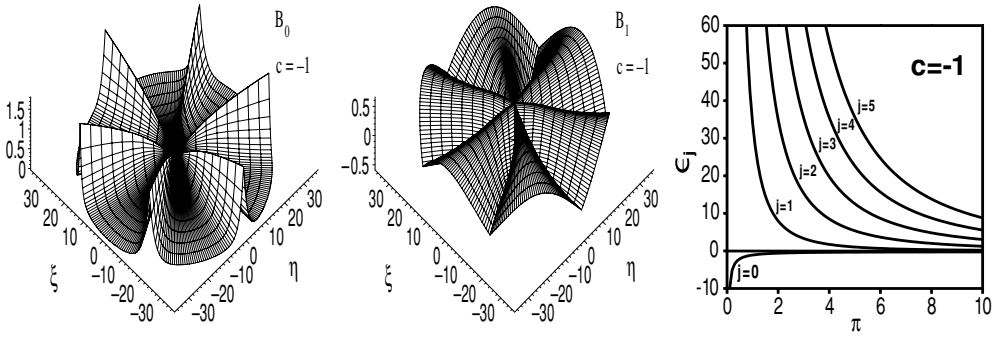

Figure 1. The first two surface functions $B_0(\rho;\theta)$ and $B_1(\rho;\theta)$ and the eigenvalues $\epsilon_0(\rho)$ and $\epsilon_j(\rho)$ $(j = 1, \ldots, 5)$ in the case of attraction $(c = -1)$.

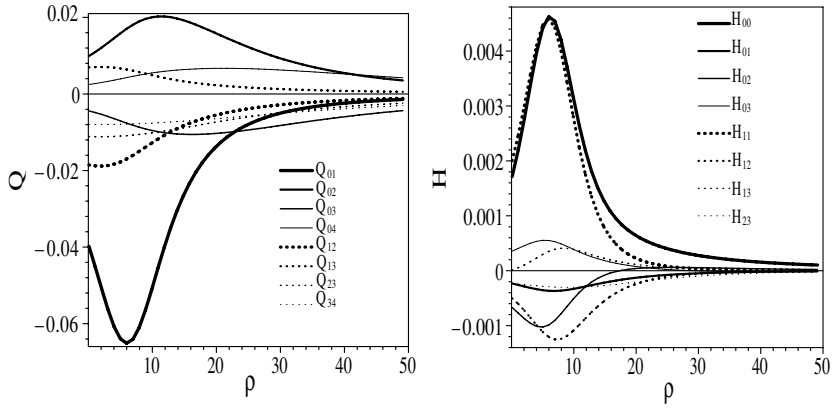

Figure 2. The matrix elements $Q_{ij}(\rho)$ and $H_{ij}(\rho)$ in the case of attraction $(c = -1)$.

$$H_{00}(\rho) = -\left(\frac{c\pi}{36}\right)^2 \frac{1}{\tilde{y}_0^6}\left[\frac{4\pi^2 y_0^4 - \tilde{y}_0^4}{4\tilde{y}_0^2} + \frac{\pi^2 y_0^2}{3}\left(\tilde{y}_0^2 + 4x\right)\right],$$

$$H_{jj}(\rho) = -\left(\frac{c\pi}{36}\right)^2 \frac{1}{\tilde{y}_j^6}\left[\frac{4\pi^2 y_j^4 - \tilde{y}_j^4}{4\tilde{y}_j^2} - \frac{\pi^2 y_j^2}{3}\left(\tilde{y}_j^2 - 4x\right)\right],$$

$$H_{0j}(\rho) = \left(\frac{c\pi}{36}\right)^2 \frac{(-1)^j y_0 y_j}{\tilde{y}_0^3 \tilde{y}_j^3}\left[2\pi(\pi x^2 + x)\left(\frac{1}{\tilde{y}_0^2} - \frac{1}{\tilde{y}_j^2}\right) + \pi + 2\pi^2 x + \frac{4\left(y_0^2 \tilde{y}_j^2 + \tilde{y}_0^2 y_j^2\right)}{\left(y_0^2 + y_j^2\right)^2}\right],$$

$$H_{ij}(\rho) = \left(\frac{c\pi}{36}\right)^2 \frac{(-1)^{i+j} y_i y_j}{\tilde{y}_i^3 \tilde{y}_j^3}\left[2\pi(\pi x^2 + x)\left(\frac{1}{\tilde{y}_i^2} + \frac{1}{\tilde{y}_j^2}\right) - \pi - 2\pi^2 x + \frac{4\left(y_i^2 \tilde{y}_j^2 + \tilde{y}_i^2 y_j^2\right)}{\left(y_i^2 - y_j^2\right)^2}\right],$$

$$\tilde{y}_0 = \sqrt{\pi\left(y_0^2 - x^2\right) - x}, \qquad \tilde{y}_j = \sqrt{\pi\left(y_j^2 + x^2\right) + x}, \qquad j = 1, 2, \ldots, \tag{16}$$

that are shown, as an example, in figure 2. The asymptotic behaviour of these matrix elements and of the potential curves are given in appendix A.

Thus, in the model described *all the effective potentials* (13) *of the set of close-coupled radial equations* (12) *are evaluated exactly* and, therefore, provide the foundation for good benchmark multichannel calculations (for example, see [19, 20, 22]).

2.2. The effective approximation for the Kantorovich method

To obtain the effective approximation for the KM, we consider the system of equations (12) and neglect the coupling of the states $|j\rangle$ which do not also involve the open channel $|0\rangle$. We introduce the so-called effective adiabatic approximation (EAA) in which we project these equations onto the two-body open channel $|0\rangle$ by means of a canonical transformation similar to that of [3, 21]. The new solution $\chi_i^{\text{new}} \equiv \chi_i^{\text{new}}(\rho)$ is connected with the solutions $\chi_j(\rho)$ of the system (12) by the relation

$$\chi_i^{\text{new}} = \sum_j T_{ij}\chi_j \approx \sum_{j,j'=0}^{j_{\max}} \langle i|\exp(\iota S^{(2)})|j'\rangle\langle j'|\exp(\iota S^{(1)})|j\rangle\chi_j. \tag{17}$$

Restricting expansions of the exponents to second order, i.e., expressing $\exp(\iota S^{(1)}) \approx 1 + \iota S^{(1)} + (\iota S^{(1)})^2/2$ and $\exp(\iota S^{(2)}) \approx 1 + \iota S^{(2)}$, we define the non-diagonal matrix elements of generator $S^{(1)}$ and $S^{(2)}$ by such a way

$$\begin{aligned} \iota S_{ij}^{(1)} &= (1-\delta_{ij})\Delta_{ij}^{-1}\left(H_{ij} + Q_{ij}\frac{\mathrm{d}}{\mathrm{d}\rho} + \frac{1}{\rho}\frac{\mathrm{d}}{\mathrm{d}\rho}\rho Q_{ij}\right), \\ \iota S_{ij}^{(2)} &= (1-\delta_{ij})2\Delta_{ij}^{-2}Q_{ij}V'_{jj}, \qquad \Delta_{ij} = \Delta_{ij}(\rho) = V_{ii} - V_{jj}, \end{aligned} \tag{18}$$

and determine the inverse operator for pair channel $|0\rangle$

$$\begin{aligned} &\chi_j = T_{j0}^{-1}\chi_0^{\text{new}}, \qquad \chi_0^{\text{new}} = \sum_j T_{0j}\chi_j, \\ &\langle 0|T|0\rangle = \langle 0|T^{-1}|0\rangle = 1 = \langle 0|0\rangle. \end{aligned} \tag{19}$$

This leads to a projection of the above system of equations onto the pair channel $|0\rangle$

$$\sum_{ij} T_{0i}(H^{\text{old}} - 2E)_{ij}T_{j0}^{-1}\chi_0^{\text{new}} = \left(H_{00}^{\text{new}} - 2E\right)\chi_0^{\text{new}} = 0, \tag{20}$$

$$\left(H_{00}^{\text{new}} - 2E\right)\chi_0^{\text{new}} = -\frac{1}{\rho}\frac{\mathrm{d}}{\mathrm{d}\rho}\frac{\rho}{\mu}\frac{\mathrm{d}\chi_0^{\text{new}}}{\mathrm{d}\rho} + \frac{\mu'}{2\mu^2\rho}\chi_0^{\text{new}} + [\hat{U}_{\text{eff}} - 2E]\chi_0^{\text{new}} = 0. \tag{21}$$

The new solution $\psi \equiv \mu^{-1/2}\chi_0^{\text{new}}(\rho)$ in such a diagonal representation satisfies the following equation,

$$(\hat{H}_{\text{eff}} - 2E)\psi \equiv -\frac{1}{\rho}(\rho\psi')' + \mu^{1/2}(\mu^{-1/2})''\psi + \mu[\hat{U}_{\text{eff}} - 2E]\psi = 0, \qquad \lim_{\rho\to 0}\rho\frac{\mathrm{d}\psi}{\mathrm{d}\rho} = 0, \tag{22}$$

where the effective potential $\hat{U}_{\text{eff}}(\rho)$ is defined as a sum of the adiabatic potential $\hat{U}_{\text{ad}}(\rho)$ and the *effective nonadiabatic correction* $\delta U(\rho)$,

$$\hat{U}_{\text{eff}}(\rho) = \hat{U}_{\text{ad}}(\rho) + \delta U(\rho), \tag{23}$$

and the modified scalar product and the adiabatic potential are defined by

$$\langle\psi|\psi\rangle = \int_0^\infty \mathrm{d}\rho\,\rho\mu\psi\psi, \qquad \hat{U}_{\text{ad}}(\rho) = \epsilon_0(\rho) + \frac{W(\rho)}{4\rho^2} + H_{00}(\rho).$$

The term $\mu(\rho)$ can be regarded as an *effective mass*, defined as the inverse of the sum of 1 and the effective mass correction $W(\rho)$:

$$\begin{aligned} &\mu^{-1}(\rho) = 1 + W(\rho), \qquad W(\rho) = -4\sum_{j=1}^{j_{\max}} Q_{0j}(\rho)Q_{j0}(\rho)\Delta_{0j}^{-1}(\rho), \\ &\delta U(\rho) = \sum_{j=1}^{j_{\max}}\left(\Delta_{0j}^{-1}V_{0j}^{(1)} + \Delta_{0j}^{-2}V_{0j}^{(2)} + \Delta_{0j}^{-3}V_{0j}^{(3)}\right). \end{aligned} \tag{24}$$

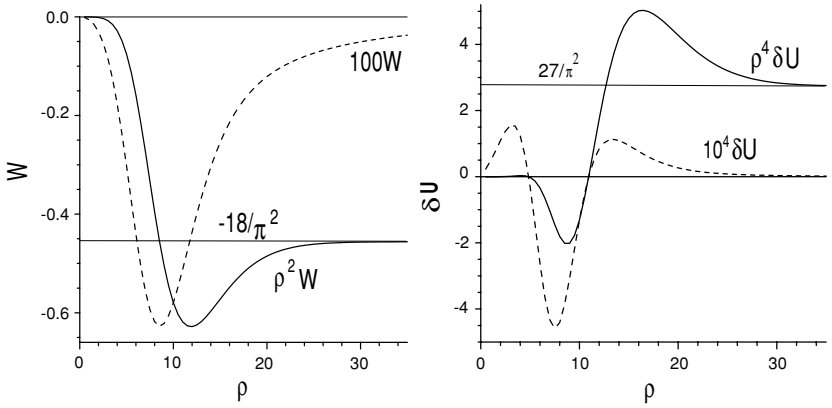

Figure 3. The effective mass correction $W(\rho)$ and the nonadiabatic correction $\delta U(\rho)$ to the effective adiabatic potential $\hat{U}_{\rm eff}(\rho)$.

Here we are using

$$V_{0j}^{(1)} = H_{0j}^2 - (Q'_{0j})^2 + 2Q_{0j}H'_{0j} - 2Q_{0j}Q''_{0j},$$
$$V_{0j}^{(2)} = H_{0j}Q_{0j}(\Sigma'_{0j} - \Delta'_{0j}) + Q_{0j}Q'_{0j}(\Sigma'_{0j} + 3\Delta'_{0j}) + Q_{0j}^2(\Sigma''_{0j} + \Delta''_{0j}),$$
$$V_{0j}^{(3)} = Q_{0j}^2(\Sigma'_{0j} + \Delta'_{0j})(\Sigma'_{0j} - 2\Delta'_{0j}),$$
$$\Delta_{0j} = \Delta_{0j}(\rho) = V_{00} - V_{jj}, \qquad \Sigma_{0j} = \Sigma_{0j}(\rho) = V_{00} + V_{jj}.$$

In the above formulae all the terms determined by (13)–(16) are the functions of ρ, and the symbol '′' denotes a derivative in ρ. Figure 3 shows the correction $W(\rho)$ to the inverse effective mass μ^{-1} and the correction $\delta U(\rho)$ to the adiabatic potential $\hat{U}_{\rm ad}(\rho)$, in the case $j_{\max} = 100$ that provides true asymptotic values at large ρ. Here, we calculate the corrections to the effective mass and potential for $\rho = \rho_m = 100$, $j_{\max} = 100$:

$$\rho^2 W(\rho) = -1.823\,83 \approx -18\pi^{-2}$$
$$\rho^4 \sum_{j=1}^{j_{\max}} \Delta_{0j}^{-1} V_{0j}^{(1)} = -0.024\,42 + 1.073\,78 + 0.049\,87 + 2.337\,62 = 3.436\,86,$$
$$\rho^4 \sum_{j=1}^{j_{\max}} \Delta_{0j}^{-2} V_{0j}^{(2)} = -0.003\,21 - 0.697\,71 + 4 \times 10^{-8} = -0.700\,93, \qquad (25)$$
$$\rho^4 \sum_{j=1}^{j_{\max}} \Delta_{0j}^{-3} V_{0j}^{(3)} = 7 \times 10^{-11},$$
$$\rho^4 \delta U(\rho) = 3.436\,86 - 0.700\,93 + 7 \times 10^{-11} = 2.735\,93 \approx 27\pi^{-2},$$

which differ from the exact asymptotic values $W_{00}^{(0)} = 1/(2\bar{\kappa}^2) = -18\pi^{-2}$ and $\delta U_{00}^{(0)} = 3/(4\bar{\kappa}^2) = 27\pi^{-2}$ obtained in (C.5), (C.6) by 6×10^{-4} and 2.6×10^{-3}, respectively.

The convergence of these series to an exact value strongly supports the use of a finite number N of basis functions (14) in the reduction of the problem (12) to the finite interval of $0 < \rho < \rho_m$, considered in section 3.

Note that the procedure of the reduction of a system of $N = j_{\max} + 1$ second-order differential equations (12) to an effective one (22), using the canonical transformations

(17)–(19) and the calculations of asymptotic values on the left-hand side of (25), was elaborated and implemented by means of the computer algebra packages REDUCE and MAPLE.

3. Reducing the problem to a finite interval

3.1. Discrete spectrum problem: the Rayleigh–Ritz variational functional

For the ground state, we used the following asymptotical behaviour of the amplitudes $\chi_j(\rho)$ of the solution of (12) at large $q\rho \geqslant q\rho_m \gg 1$ [22]:

$$\chi_0(\rho) \to C_0 \frac{\exp(-\bar{q}\rho)}{\sqrt{\rho}}, \qquad \chi_j(\rho) \to C_j \frac{\exp(-\bar{q}\rho)}{\rho^3}. \tag{26}$$

From these relations we can obtain the homogeneous third-type boundary condition for large $q\rho_m \gg 1$

$$\begin{aligned} \rho_m \frac{\mathrm{d}\chi_0(\rho_m)}{\mathrm{d}\rho} &= -\left(\frac{1}{2} + \bar{q}\rho_m\right)\chi_0(\rho_m, \bar{q}) = -f_0(\rho_m, \bar{q})\chi_0(\rho_m), \\ \rho_m \frac{\mathrm{d}\chi_j(\rho_m)}{\mathrm{d}\rho} &= -(3 + \bar{q}\rho_m)\chi_j(\rho_m) = -f_j(\rho_m, \bar{q})\chi_j(\rho_m). \end{aligned} \tag{27}$$

Here $\bar{q}^2 = -2E(\bar{q}) - \pi^2/36 \geqslant 0$ and $E < 0$ is the unknown eigenvalue.

Using these formulae, we devise the following iteration process for each nth step $n = 1, 2, \ldots$: we solve (12) to find functions $\boldsymbol{\chi}^{(n)}$ satisfying the boundary problem:

$$\begin{aligned} &(H - 2E(\bar{q}^{(n-1)}))\boldsymbol{\chi}^{(n)} = 0, \qquad \lim_{\rho\to 0} \rho \frac{\mathrm{d}\boldsymbol{\chi}^{(n)}}{d\rho} = 0, \\ &\rho_m \frac{\mathrm{d}\boldsymbol{\chi}^{(n)}(\rho_m)}{\mathrm{d}\rho} = -\boldsymbol{f}(\rho_m, \bar{q}^{(n-1)})\boldsymbol{\chi}^{(n)}(\rho_m), \end{aligned} \tag{28}$$

where the energy $E(\bar{q}) = E(\bar{q}^{(n-1)})$ is known from the previous $n-1$th step. To find the value $E(\bar{q}^{(n)})$, we then use the iteration formula starting with some initial $\bar{q}^{(0)}$:

$$2E(\bar{q}^{(n)}) = \mathcal{R}(\boldsymbol{\chi}^{(n-1)}, \bar{q}^{(n-1)}), \tag{29}$$

which follows from the Rayleigh–Ritz variational functional

$$\mathcal{R}(\boldsymbol{\chi}, \bar{q}) = \frac{\int_0^{\rho_m} \sum_{i,j=0}^{N-1} [\chi H \chi]_{ij} \rho \,\mathrm{d}\rho + \sum_{j=0}^{N-1} f_j(\rho_m, \bar{q})\chi_j^2(\rho_m)}{\int_0^{\rho_m} \sum_{j=0}^{N-1} \chi_j^2(\rho)\rho \,\mathrm{d}\rho}, \tag{30}$$

where

$$[\chi H \chi]_{ij} = \chi_i'(\rho)\chi_j'(\rho)\delta_{ij} + \chi_i(\rho)V_{ij}(\rho)\chi_j(\rho) + Q_{ij}(\rho)[\chi_i(\rho)\chi_j'(\rho) - \chi_i'(\rho)\chi_j(\rho)].$$

To solve eigenvalue problem for the EAA, we devise also the following iteration process for each nth step $n = 1, 2, \ldots$: we solve (22) to find functions $\psi^{(n)}$ satisfying the boundary problem:

$$\begin{aligned} &(\hat{H}_{\mathrm{eff}} - 2E(\bar{q}^{(n-1)}))\psi^{(n)} = 0, \qquad \lim_{\rho\to 0} \rho \frac{\mathrm{d}\psi^{(n)}}{d\rho} = 0, \\ &\rho_m \frac{\mathrm{d}\psi^{(n)}(\rho_m)}{\mathrm{d}\rho} = -f_0(\rho_m, \bar{q}^{(n-1)})\psi^{(n)}(\rho_m), \end{aligned} \tag{31}$$

where the energy $E(\bar{q}) = E(\bar{q}^{(n-1)})$ is known from the previous $n-1$th step. To find the value $E(\bar{q}^{(n)})$, we then use the iteration formula starting with some initial $\bar{q}^{(0)}$:

$$2E(\bar{q}^{(n)}) = \mathcal{R}_{\mathrm{eff}}(\psi^{(n-1)}, \bar{q}^{(n-1)}), \tag{32}$$

which follows from the Rayleigh–Ritz variational functional

$$\mathcal{R}_{\rm eff}(\psi,\bar{q}) = \frac{\int_0^{\rho_m} \psi\hat{H}_{\rm eff}\psi\rho\,{\rm d}\rho + f_0(\rho_m,\bar{q})\psi^2(\rho_m)}{\int_0^{\rho_m}\psi^2(\rho)\mu(\rho)\rho\,{\rm d}\rho}, \tag{33}$$

where

$$\psi\hat{H}_{\rm eff}\psi = \psi'(\rho)\psi'(\rho) + [\mu^{1/2}(\rho)(\mu^{-1/2}(\rho))'' + \mu(\rho)\hat{U}_{\rm eff}(\rho)]\psi^2(\rho).$$

We recall that a variational method was originally applied by Lord Rayleigh in 1873 to the computation of vibration frequencies of mechanical systems, and developed to solve an eigenvalue problem by Ritz [24]. A further formulation of the variational method, for quantum scattering theory, was proposed by Hulthèn [25] and will be considered in the next subsection.

3.2. Continuous spectrum problem: the Hulthèn variational functional

For the elastic scattering states, with a given value for the energy $\pi^2/36 < 2E(q) = q^2 - \pi^2/36 \leqslant 0$, we rewrite the problem (12) in the form

$$(H-q^2)\boldsymbol{\chi} \equiv -\mathbf{I}\frac{1}{\rho}\frac{\rm d}{{\rm d}\rho}\rho\frac{{\rm d}\boldsymbol{\chi}}{{\rm d}\rho} + \mathbf{V}\boldsymbol{\chi} + \mathbf{Q}\frac{{\rm d}\boldsymbol{\chi}}{{\rm d}\rho} + \frac{1}{\rho}\frac{{\rm d}\rho\mathbf{Q}\boldsymbol{\chi}}{{\rm d}\rho} - 2E(q)\mathbf{I}\boldsymbol{\chi}, \qquad \lim_{\rho\to 0}\rho\frac{{\rm d}\boldsymbol{\chi}}{{\rm d}\rho} = 0. \tag{34}$$

For large $\rho \geqslant \rho_m \gg N$ the amplitudes $\chi_j(\rho)$ of the solution of the system of N equations satisfy the following asymptotic conditions:

$$\chi_0^{\rm as}(\rho) = F_0(\rho,q,\delta) + O(\rho^{-11/2}), \qquad \chi_j^{\rm as}(\rho) = F_j(\rho,q,\delta) + O(\rho^{-5}).$$

Here for $q > 0$, $q\rho \gg 1$:

$$\begin{aligned} F_0(\rho,q,\delta) &= \frac{\sin(q\rho+\delta)}{\sqrt{q\rho}} - \frac{279\,936q\cos(q\rho+\delta)(4(N-1)^3 - N + 1)}{\pi^6\rho^4\sqrt{q\rho}}, \\ F_j(\rho,q,\delta) &= 7776(2j-1)(-1)^j\left(\frac{2\sqrt{q}\cos(q\rho+\delta)}{\pi^4\rho^3} + \frac{108\sqrt{q}\cos(q\rho+\delta)}{\pi^6\rho^4}\right. \\ &\quad \left. + \frac{3(120q^2-\pi^2)\sin(q\rho+\delta)}{\pi^6\sqrt{q}\rho^4}\right), \end{aligned} \tag{35}$$

and for $q = 0$, $\rho \gg 1$:

$$\begin{aligned} F_0(\rho,0,a) &= \sqrt{\rho} + \frac{a}{\sqrt{\rho}} + \frac{979\,776(4(N-1)^3 - N + 1)}{5\pi^6\rho^4\sqrt{\rho}}, \\ F_j(\rho,0,a) &= 7776(2j-1)(-1)^j\left(-\frac{1}{\pi^4\rho^3} - \frac{3(18+a\pi^2)}{\pi^6\rho^4}\right). \end{aligned} \tag{36}$$

Using these formulae, we devise the following iteration process for each nth step $n = 1, 2, \ldots$: we solve (34) to find functions $\boldsymbol{\chi}^{(n)}$ satisfying the boundary problem:

$$\begin{aligned} &(H-q^2)\boldsymbol{\chi}^{(n)} = 0, \qquad \lim_{\rho\to 0}\rho\frac{{\rm d}\boldsymbol{\chi}^{(n)}}{{\rm d}\rho} = 0, \\ &\rho_m\frac{{\rm d}\boldsymbol{\chi}^{(n)}(\rho_m)}{{\rm d}\rho} = \rho_m\frac{{\rm d}\boldsymbol{F}(\rho_m,q,b^{(n-1)})}{{\rm d}\rho}, \end{aligned} \tag{37}$$

where the phase shift $b = \delta \equiv \delta^{(n-1)}$ at $q \neq 0$ or for the scattering length $b = a \equiv a^{(n-1)}$ at $q = 0$ are known from the previous $n-1$th step. To find the value $b^{(n)}$, we then use the iteration formula starting with some initial $b^{(0)}$:

$$b^{(n)} = b^{(n-1)} + \mathcal{H}(\boldsymbol{\chi}^{(n-1)}, q, b^{(n-1)}), \tag{38}$$

which follows from the Hulthèn variational functional [23]

$$\mathcal{H}(\chi, q, b) = \int_0^{\rho_m} \sum_{i,j=0}^{N-1} [\chi(H - q^2)\chi]_{ij}\rho \, \mathrm{d}\rho - \frac{1}{2}\rho_m \sum_{j=0}^{N-1} \frac{\mathrm{d}F_j^2(\rho_m, q, b)}{\mathrm{d}\rho} + \rho_m \sum_{i,j=0}^{N-1} Q_{ij}(\rho_m) F_i(\rho_m, q, b) F_j(\rho_m, q, b), \tag{39}$$

where

$$[\chi(H - q^2)\chi]_{ij} = \chi_i'(\rho)\chi_j'(\rho)\delta_{ij} + \chi_i(\rho)V_{ij}(\rho)\chi_j(\rho) - 2E(q)\chi_i(\rho)\chi_j(\rho)\delta_{ij} + Q_{ij}(\rho)[\chi_i(\rho)\chi_j'(\rho) - \chi_i'(\rho)\chi_j(\rho)].$$

Note that the above iterative procedures usually converge after $n \sim 7$–8 iterations.

3.3. Continuous spectrum problem: the effective approximation

For the elastic scattering states with the given value $2E(q) = q^2 - \pi^2/36 < 0$ we rewrite the problem (22) in the form

$$(\hat{H}_{\text{eff}} - q^2)\psi \equiv -\frac{1}{\rho}(\rho\psi')' + \mu^{1/2}(\mu^{-1/2})''\psi + \mu[\hat{U}_{\text{eff}} - 2E(q)]\psi = 0, \qquad \lim_{\rho\to 0} \rho\frac{\mathrm{d}\psi}{\mathrm{d}\rho} = 0. \tag{40}$$

For function $\chi^{\text{eff}} = (\rho\mu)^{1/2}\psi$ this equation has a conventional form

$$\left(\frac{\mathrm{d}}{\mathrm{d}\rho}\mu^{-1}(\rho)\frac{\mathrm{d}}{\mathrm{d}\rho} - U_{\text{eff}}(\rho) + q^2\right)\chi_{00}^{\text{eff}}(\rho) = 0, \tag{41}$$

where the effective potential $U_{\text{eff}}(\rho)$ is defined by

$$U_{\text{eff}}(\rho) = V_{00}(\rho) + \delta U(\rho) - \frac{1}{4\rho^2} - \epsilon_0^{(0)}. \tag{42}$$

For large values of ρ, using asymptotic values $W_{00}^{(N)}(\rho) = \rho^2 W(\rho)$ and $\delta U_{00}^{(N)}(\rho) = \rho^4 \delta U(\rho)$ from (24), it reduces to the following one:

$$\left(-\frac{\mathrm{d}}{\mathrm{d}\rho}\left(1 + \frac{W_{00}^{(N)}}{\rho^2}\right)\frac{\mathrm{d}}{\mathrm{d}\rho} + \frac{\delta U_{00}^{(N)}}{\rho^4} - q^2\right)\bar{\chi}_{00}^{\text{as}}(\rho) = 0, \tag{43}$$

and to an accuracy of the order $O(\rho^{-4})$, equation (41) reads

$$\left[\frac{\mathrm{d}^2}{\mathrm{d}\rho^2} - \frac{2W_{00}^{(N)}}{\rho^3}\frac{\mathrm{d}}{\mathrm{d}\rho} + q^2\left(1 - \frac{W_{00}^{(N)}}{\rho^2}\right) - \frac{\delta U_{00}^{(N)}}{\rho^4}\right]\bar{\chi}_{00}^{\text{as}}(\rho) = 0. \tag{44}$$

For $qW_{00}^{(N)}/(2\rho) \ll 1$, the continuous spectrum solutions of equation (41) can be put into the form

$$\bar{\chi}_{00}^{\text{as}}(\rho) \sim \sin\left[q\rho\left(1 - \frac{W_{00}^{(N)}}{2\rho^2}\right) + \delta^{(N)}\right] \approx \sin(q\rho + \delta^{(N)}) - q\frac{W_{00}^{(N)}}{2\rho}\cos(q\rho + \delta^{(N)}), \tag{45}$$

where $\delta^{(N)} \equiv \delta^{(N)}(q)$ is the phase shift of the elastic scattering in the open pair channel $|0\rangle$, below the main three-body threshold, $E = 0$. The required asymptotic solutions such as (35),

(36) are evaluated by a direct substitution of asymptotics (45) and the matrix elements from appendices A and B into equation (17).

Using these formulae, we devise the following iteration process for each nth step $n = 1, 2, \ldots$: we solve (40) to find functions $\psi^{(n)}$ satisfying the boundary problem:

$$\begin{aligned} &(\hat{H}_{\rm eff} - q^2)\psi^{(n)} = 0, \qquad \lim_{\rho\to 0} \rho \frac{{\rm d}\psi^{(n)}}{{\rm d}\rho} = 0, \\ &\rho_m \frac{{\rm d}\psi^{(n)}(\rho_m)}{{\rm d}\rho} = \rho_m \frac{{\rm d}F_0(\rho_m, q, \delta^{(n-1)})}{{\rm d}\rho}, \end{aligned} \tag{46}$$

where the phase shift $\delta \equiv \delta^{(n-1)}$ is known from the previous $n-1$th step. To find the value $\delta^{(n)}$, we then use the iteration formula starting with some initial $\delta^{(0)}$:

$$\delta^{(n)} = \delta^{(n-1)} + \mathcal{H}_{\rm eff}(\psi^{(n-1)}, q, \delta^{(n-1)}), \tag{47}$$

which follows from the Hulthèn variational functional like (39) (see (35))

$$\mathcal{H}_{\rm eff}(\psi, q, \delta) = \int_0^{\rho_m} \psi(\hat{H}_{\rm eff} - q^2)\psi\rho \, {\rm d}\rho - \frac{1}{2}\rho_m \frac{{\rm d}F_0^2(\rho_m, q, \delta)}{{\rm d}\rho}, \tag{48}$$

where

$$\psi(\hat{H}_{\rm eff} - q^2)\psi = \psi'(\rho)\psi'(\rho) + [\mu^{1/2}(\rho)(\mu^{-1/2}(\rho))'' + \mu(\rho)\hat{U}_{\rm eff}(\rho) - 2\mu(\rho)E(q)]\psi^2(\rho).$$

Remembering that $\rho^2 = \xi^2 + \eta^2$ and $\xi \sim \rho(1 - \eta^2/(2\rho^2))$ in the asymptotic region $\eta/\rho \ll 1$ one should introduce the following definition of the *mean position* operator in the new representation $\chi^{\rm new} = T\chi$

$$\rho^{\rm new}_{\rm mean} = \langle \chi^{\rm new} | \hat{\rho}^{\rm new}_{\rm mean} | \chi^{\rm new} \rangle = \langle \chi | T^{-1} \hat{\rho}^{\rm new}_{\rm mean} T | \chi \rangle = \langle \chi | \hat{\rho}_{\rm mean} | \chi \rangle = \rho_{\rm mean}.$$

Here the *mean position* operator $\hat{\rho}^{\rm new}_{\rm mean} = \rho$ plays the role of the Jacobi coordinate ξ in the new representation $\chi^{\rm new}$, i.e. a delocalization of ξ is contained in the new radial functions $\chi^{\rm new} = T\chi$. In the old representation χ the mean position operator $\hat{\rho}_{\rm mean}$ is defined as

$$\hat{\rho}_{\rm mean} = T^{-1}\hat{\rho}^{\rm new}_{\rm mean} T = T^{-1}\rho T = \rho + \delta\hat{\rho},$$

where $\delta\hat{\rho}$ is a delocalization of the Jacobi coordinate ξ, that in the asymptotic region $\eta/\rho \ll 1$ has the order of $\eta^2/(2\rho)$, i.e.

$$\hat{\rho}_{\rm mean} \to T^{-1}\rho T \approx \langle \xi \rangle.$$

Note, transformation (17) changes only form of radial solutions, and the Jacobi coordinates ξ restoring only in total expansion (9) of the wavefunction (see (C.11)–(C.13)). So, if we omit nonadiabatic term in equation (44) and take the adiabatic behaviour

$$\chi^{\rm ad} \sim \sin(q\rho + \delta^{\rm ad}),$$

we then find the obvious difference between the true phase shift δ, Nth approximation $\delta^{(N)}$ and the adiabatic phase shift $\delta^{\rm ad}$,

$$\delta^{(N)} = \delta^{\rm ad} - q\frac{W^{(N)}_{00}}{2\rho}, \qquad \delta = \lim_{N\to\infty} \delta^{(N)} = \delta^{\rm ad} + q\frac{\langle 0|\eta^2|0\rangle}{2\rho}, \tag{49}$$

in accordance with equations (C.5) and (C.15).

4. High-order approximations of the finite-element method

In order to solve numerically the Sturm–Liouville problems for equations (28) or (31) (for the discrete spectrum problem with the Rayleigh–Ritz variational functional) and (37) or (46) (for the continuous spectrum problem with the Hulthèn variational functional) the high-order approximations of the finite element method (FEM) [26, 27] elaborated in our previous paper [28] have been used. Such high-order approximations of the FEM have been proved [28] to be very accurate, stable and effective for a wide set of quantum-mechanical problems. Computational schemes of the high order of accuracy are derived from the Rayleigh–Ritz variational functional (30) or (33) and the Hulthèn variational functional (38) or (47) on the basis of the finite element method. The general idea of the FEM in one-dimensional space is to subdivide interval $[0, \rho_m]$ into many small domains called elements. The size and shape of elements can be defined very freely so that physical properties can be taken into account.

Now we cover the interval $\Delta = [0, \rho_{\mathrm{m}}]$ by a system of subintervals $\Delta_j = [\rho_{j-1}, \rho_j]$ in such a way that $\Delta = \bigcup_{j=1}^{n} \Delta_j$, where n is the number of subintervals. In each interval Δ_j determine the following nodes:

$$\rho_{j,r}^p = \rho_{j-1} + \frac{h_j}{p} r, \qquad h_j = \rho_j - \rho_{j-1}, \qquad r = 0, 1, \ldots, p,$$

and the Lagrange elements $\{\phi_{j,r}^p(\rho)\}_{r=0}^p$

$$\phi_{j,r}^p(\rho) = \frac{(\rho - \rho_{j,0}^p)(\rho - \rho_{j,1}^p)\cdots(\rho - \rho_{j,r-1}^p)(\rho - \rho_{j,r+1}^p)\cdots(\rho - \rho_{j,p}^p)}{(\rho_{j,r}^p - \rho_{j,0}^p)(\rho_{j,r}^p - \rho_{j,1}^p)\cdots(\rho_{j,r}^p - \rho_{j,r-1}^p)(\rho_{j,r}^p - \rho_{j,r+1}^p)\cdots(\rho_{j,r}^p - \rho_{j,p}^p)}.$$

By means of the Lagrange elements $\phi_{j,r}^p(\rho)$, at the each node $\rho_{j,r}^p$ we define the function $N_l(\rho)$ in the the following way:

$$N_l(\rho) = \begin{cases} \begin{cases} \phi_{1,0}^p(\rho), & \rho \in \Delta_1, \\ 0, & \rho \notin \Delta_1, \end{cases} & l = 0, \\ \begin{cases} \phi_{j,r}^p(\rho), & \rho \in \Delta_j, \\ 0, & \rho \notin \Delta_j, \end{cases} & l = r + p(j-1), \quad r = 1, 2, \ldots, p-1, \\ \begin{cases} \phi_{j,p}^p(\rho), & \rho \in \Delta_j, \\ \phi_{j+1,0}^p(\rho), & \rho \in \Delta_{j+1}, \\ 0, & \rho \notin \Delta_j \bigcup \Delta_{j+1}, \end{cases} & l = jp, \quad j = 1, 2, \ldots, n-1, \\ \begin{cases} \phi_{n,p}^p(\rho), & \rho \in \Delta_n, \\ 0, & \rho \notin \Delta_n, \end{cases} & l = np. \end{cases}$$

The functions $\{N_l^p(\rho)\}_{l=0}^L$, $L = np$, form a basis in the space of polynomials of the p-th order. Now, we approximate each function $\chi_\mu(\rho)$ of the global function $\chi^T(\rho) = (\chi_0(\rho), \chi_1(\rho), \ldots, \chi_{N-1}(\rho))$ by a finite sum of local functions $N_l^p(\rho)$

$$\chi_\mu(\rho) = \sum_{l=0}^{L} \chi_\mu^l N_l^p(\rho), \qquad \chi_\mu^l \equiv \chi_\mu^l(\rho_{j,r}^p), \tag{50}$$

and substitute expansion (50) into the functional (30) or (33). From the minimum condition [26, 27] for this functional we obtain that vector solution $\boldsymbol{\chi}^h$ is the eigenvector of the generalized algebraic problem

$$(\mathbf{K}^p + \mathbf{B})\boldsymbol{\chi}^h = E^h \mathbf{M}^p \boldsymbol{\chi}^h. \tag{51}$$

Here $\mathbf{B}$ is a diagonal matrix and has zero elements, except last N elements, that are defined by the boundary conditions (28) or (31):

$$B_{LN-N+\mu, LN-N+\mu} = f_{\mu-1}(\rho_m, q^h), \qquad \mu = 1, 2, \ldots, N.$$

To solve the scattering problem at a fixed value of the energy $E(q)$ it is necessary to consider the right-hand-side problem with respect to vector solution χ^h, which follows from the stationary condition [23] for the functional (39) or (48):

$$(\mathbf{K}^p - E(q)\mathbf{M}^p)\chi^h = \mathbf{B}. \tag{52}$$

Here $\mathbf{B}$ is a vector and has zero elements, except last N elements, that are defined by the boundary conditions (37) or (46):

$$B_{LN-N+\mu} = \rho_m \frac{\mathrm{d}F_{\mu-1}(\rho_m, q, b^h)}{\mathrm{d}\rho} - \rho_m \sum_{\nu=1}^{N} Q_{\mu-1\nu-1} F_{\nu-1}(\rho_m, q, b^h), \qquad \mu = 1, 2, \ldots, N.$$

The following estimations for FEM eigenfunctions of problem (30) or (33) are valid [26]:

$$\left|E_m^h - E_m\right| \leqslant c_1(E_m)h^{2p}, \qquad \left\|\chi_m^h(\rho) - \chi_m(\rho)\right\|_0 \leqslant c_2(E_m)h^{p+1}, \tag{53}$$

where h is the maximal step of the finite-element grid, m is the number of the corresponding solutions, and constants c_1 and c_2 do not depend on step h. The similar estimations take place for approximate values of the phase shift δ^h and scattering length a^h, which follow from the corresponding approximation of the Hulthèn variational functional (39) or (48). The stiffness matrix $\mathbf{K}^p$ and the mass matrix $\mathbf{M}^p$ are symmetric and have a banded structure, and $\mathbf{M}^p$ matrix is also positively defined. They have the following form,

$$\mathbf{K}^p = \sum_{j=1}^{n} \mathbf{k}_j^p, \qquad \mathbf{M}^p = \sum_{j=1}^{n} \mathbf{m}_j^p, \tag{54}$$

where the local on the element Δ_j matrices $\mathbf{k}_j^p$ and $\mathbf{m}_j^p$ are calculated by the formulae

$$\begin{aligned}
\left(\mathbf{k}_j^p\right)_{\mu\nu}^{qr} &= \int_{-1}^{+1} \left\{ \delta_{\mu\nu} \frac{4}{h_j^2} \left(\phi_{j,q}^p\right)'(\rho) \left(\phi_{j,r}^p\right)'(\rho) + V_{\mu-1\nu-1}(\rho)\phi_{j,q}^p(\rho)\phi_{j,r}^p(\rho) \right. \\
&\quad \left. + Q_{\mu-1\nu-1}(\rho)\left[\phi_{j,q}^p(\rho)\left(\phi_{j,r}^p\right)'(\rho) - \left(\phi_{j,q}^p\right)'(\rho)\phi_{j,r}^p(\rho)\right]\frac{2}{h_j} \right\} \rho \frac{h_j}{2}\,\mathrm{d}\eta, \\
\left(\mathbf{m}_j^p\right)_{\mu\nu}^{qr} &= \delta_{\mu\nu} \int_{-1}^{+1} \phi_{j,q}^p(\rho)\phi_{j,r}^p(\rho)\rho \frac{h_j}{2}\,\mathrm{d}\eta, \\
&\quad \rho = \rho_{j-1} + 0.5h_j(1+\eta), \quad q, r = 0, 1, \ldots, p, \quad \mu, \nu = 1, 2, \ldots, N.
\end{aligned} \tag{55}$$

Now let us note by η_g and w_g, $g = 0, \ldots, p$, the Gaussian nodes and weights in the interval $[-1, 1]$. Then the integrals given above are calculated as

$$\begin{aligned}
\left(\mathbf{k}_j^p\right)_{\mu\nu}^{qr} &= \sum_{g=0}^{p} \left\{ \delta_{\mu\nu} \frac{4}{h_j^2} \left(\phi_{j,q}^p\right)'(\rho_g) \left(\phi_{j,r}^p\right)'(\rho_g) + V_{\mu-1\nu-1}(\rho_g)\phi_{j,q}^p(\rho_g)\phi_{j,r}^p(\rho_g) \right. \\
&\quad \left. + Q_{\mu-1\nu-1}(\rho_g)\left[\phi_{j,q}^p(\rho_g)\left(\phi_{j,r}^p\right)'(\rho_g) - \left(\phi_{j,q}^p\right)'(\rho_g)\phi_{j,r}^p(\rho_g)\right]\frac{2}{h_j} \right\} \rho_g \frac{h_j}{2} w_g, \\
\left(\mathbf{m}_j^p\right)_{\mu\nu}^{qr} &= \sum_{g=0}^{p} \delta_{\mu\nu}\phi_{j,q}^p(\rho_g)\phi_{j,r}^p(\rho_g)\rho_g \frac{h_j}{2} w_g,
\end{aligned} \tag{56}$$

where $\rho_g = \rho_{j-1} + 0.5h_j(1+\eta_g)$.

Following this way we have the strategy: as we know analytically all functions V_{ij} and Q_{ij} first we choose the FEM grid, then we calculate these matrix elements in the Gaussian points and finally evaluate the integrals. This allows us to organize the calculation scheme

Table 1. Convergence of the KM for the calculated double energy values $2E_b^h$ to exact ground-state double energy $2E_b^{\text{exact}} = -\pi^2/9$ and the differences $\Delta E = 2E_b^h - 2E_b^{\text{exact}}$ versus the number of equations. The first column shows the number of equations N, the second and third ones display the calculated values and the differences in quadruple (*quad*) precision. The fourth and fifth columns display the same ones for the double (*double*) precision. The underlined significant digits are marked to show a difference with respect to the exact values that are shown without any underlining. The exact ground-state double energy $2E_b^{\text{exact}}$ is shown with 15 significant digits. The factor x in the brackets denotes 10^x.

N	$2E_{KM}^{\text{quad}}$	$\Delta E_{KM}^{\text{quad}}$	$2E_{KM}^{\text{double}}$	$\Delta E_{KM}^{\text{double}}$
1	−1.096 442 612 726 35	1.801(−04)	−1.096 442 612 725 82	1.801(−04)
2	−1.096 619 949 281 73	2.762(−06)	−1.096 619 949 281 15	2.762(−06)
3	−1.096 622 441 487 76	2.697(−07)	−1.096 622 441 486 97	2.697(−07)
4	−1.096 622 657 101 71	5.413(−08)	−1.096 622 657 100 61	5.413(−08)
5	−1.096 622 695 292 57	1.594(−08)	−1.096 622 695 291 63	1.594(−08)
6	−1.096 622 705 282 40	5.949(−09)	−1.096 622 705 282 09	5.950(−09)
10	−1.096 622 710 835 39	3.967(−10)	−1.096 622 710 834 63	3.979(−10)
20	−1.096 622 711 221 15	1.099(−11)	−1.096 622 711 220 37	1.245(−11)
30	−1.096 622 711 230 76	1.390(−12)	−1.096 622 711 229 24	3.276(−12)
35	−1.096 622 711 231 51	6.357(−13)	−1.096 622 711 229 60	3.194(−12)
40	−1.096 622 711 231 82	3.232(−13)	−1.096 622 711 229 40	3.361(−12)
50	−1.096 622 711 232 04	1.046(−13)	−1.096 622 711 228 27	4.427(−12)
70	−1.096 622 711 232 13	1.957(−14)		
$2E_b^{\text{exact}}$	−1.096 622 711 232 15		−1.096 622 711 232 15	

as follows: let us consider the system of N equations. We evaluate the values of all matrix elements for these N equations in the Gaussian nodes and store them on the external file. Then we use it to investigate the convergence rate of the Kantorovich expansion as a function of number of equations.

From the above estimates one can see that we have a very high accuracy for calculations of both the bound state and scattering problems, i.e., the eigenvalues and phase shifts, and corresponding wavefunctions. In this point of view the main error in the solution depends only on the number of equations N and on the used computer precision.

5. Numerical results

Here we study the convergence rate of the KM as a function of the number, N, of the equations of the system (12). The problem under consideration is a good test for various (numerical) methods because it has analytical solutions for both the discrete and the continuous spectra. We begin by considering the eigenvalue problem in the case of $\rho_m = 50$. We use the 1000 finite elements of fourth order. The finite element grid consists of 4001 nodes. We consider the calculations in double and quadruple precision.

The numerical calculations are performed on 2 Alpha 21264, 750 MHz, 2 GB ram with elf 64 bit LSB executable, and using a Compaq (Fortran 77, with Compaq extensions) compiler suitable for the Linux Alpha systems. We use data types REAL*8 and REAL*16 that yield 15 and 33 significant digits respectively, and call them 'double precision' and 'quadruple precision', from the point of view of calculations performed on a conventional PC.

In table 1 the differences $\Delta E = 2E^h - 2E_b^{\text{exact}}$, of the calculated values of the energy $2E^h$ from the known exact value $2E_b^{\text{exact}}$, i.e., upper bound estimates $\Delta E > 0$ to the exact energy $2E_b^{\text{exact}} = -\pi^2/9$ of the bound state, are shown for each case. One can see that, using

Table 2. Convergence of the KM for the calculated double energy values $2E_b^h$, $2E_{hb}^h$ to exact ground and half-bound double energy $2E_b^{\rm exact} = -\pi^2/9$, $2E_{hb}^{\rm exact} = -\pi^2/36$ and the differences $\Delta E_b = 2E_b^h - 2E_b^{\rm exact}$, $\Delta E_{hb} = 2E_{hb}^h - 2E_{hb}^{\rm exact}$ versus the number of equations. The first column shows the number of sums N, the second and forth ones display the calculated values, the third and fifth ones display the differences (in double precision), respectively. The underline significant digits are marked to show a difference with respect to true ones that are shown without any underlining. The exact ground-state and half-bound double energies $2E_b^{\rm exact}$, $2E_{hb}^{\rm exact}$ are shown in the last arrow with the 12 significant digits. The factor x in the brackets denotes 10^x.

N	$2E_b^h$	ΔE_b	$2E_{hb}^h$	ΔE_{hb}
1	−1.096 442 612 72	1.801(−04)	−0.274 155 329 73	3.480(−07)
2	−1.096 632 243 01	−9.532(−06)	−0.274 155 649 73	2.807(−08)
3	−1.096 634 793 13	−1.208(−05)	−0.274 155 674 00	3.802(−09)
4	−1.096 635 011 40	−1.230(−05)	−0.274 155 677 60	1.981(−10)
5	−1.096 635 049 91	−1.234(−05)	−0.274 155 678 56	−7.549(−10)
6	−1.096 635 059 96	−1.235(−05)	−0.274 155 678 91	−1.104(−09)
10	−1.096 635 065 54	−1.235(−05)	−0.274 155 679 22	−1.414(−09)
100	−1.096 635 065 94	−1.235(−05)	−0.274 155 679 28	−1.480(−09)
$2E^{\rm exact}$	−1.096 622 711 23		−0.274 155 677 80	

quadruple precision, the KM monotonically converges to the exact values, while in the double precision this is only true for about 35 equations.

Note that in the solution of the algebraic eigenvalue problem, we use the subspace iteration method (SIM) with a fixed shift of the spectrum [27]. The main step here is to find the solutions of systems of linear algebraic equations using a Cholesky decomposition. For example, when $N = 50$ the system consists of 200 050 equations! This can only be solved in a stable manner when using our quadruple precision.

As is well known, solving the eigenvalue problem for a system (12) of N equations with the help of the SIM based on the functional (30), yields only upper bounds for the energy values. However, using the effective approximation (22)–(24), i.e., a specially truncated system (12) reduced to a diagonal form, we can calculate both the upper and lower bounds to the energy $2E_b^{\rm exact}$ of the bound state and $2E_{hb}^{\rm exact} \equiv 2E(0) = \epsilon_0^{(0)} = -\pi^2/36$ of the half-bound state, as a function of the number N of equations taken into account. With this aim, we solve the eigenvalue problem for the half-bound state estimation from equation (22) in the case of $\rho_m = 2000$ with the help of the SIM based on the functional (33). We use the 4000 finite elements of fourth order. The finite element grid consists of 16 001 nodes. We consider the calculations in the double precision on the finite element grid {0 (2000) 500 (2000) 2000}, where the number in brackets denote the number of finite elements in the subintervals. In table 2, we show the calculated values of the energy $2E_b^h$ and $2E_{hb}^h$ that yield the upper and low estimations of the exact ones $2E_b^{\rm exact}$ and $2E_{hb}^{\rm exact}$ versus the number, N. We show also the values of the difference, $\Delta E_{hb} = 2E_{hb}^h - 2E_{hb}^{\rm exact}$ and $\Delta E_b = 2E_b^h - 2E_b^{\rm exact}$ versus the number, N, of the corresponding upper bounds (ΔE_b, $\Delta E_{hb} > 0$) and lower bounds (ΔE_b, $\Delta E_{hb} < 0$) compared to the exact energies $2E_b^{\rm exact}$ of ground state and $2E_{hb}^{\rm exact}$ of the half-bound state. The change of a sign of this difference, when passing from $N = 1$ to $N = 2$, implies the existence of this ground-state and passing from $N = 4$ to $N = 5$, implies the existence of this half-bound state, respectively. Thus, we have shown that the half-bound state exists, as follows from the numerical upper and lower estimates that we have obtained for its energy. This means that an additional $\pi/2$ should appear in Levinson's theorem, which corresponds to the exact phase shift in equation (8), i.e., $\delta^{\rm exact} = \pi + \pi/2$ at $q = 0$, derived in the previous

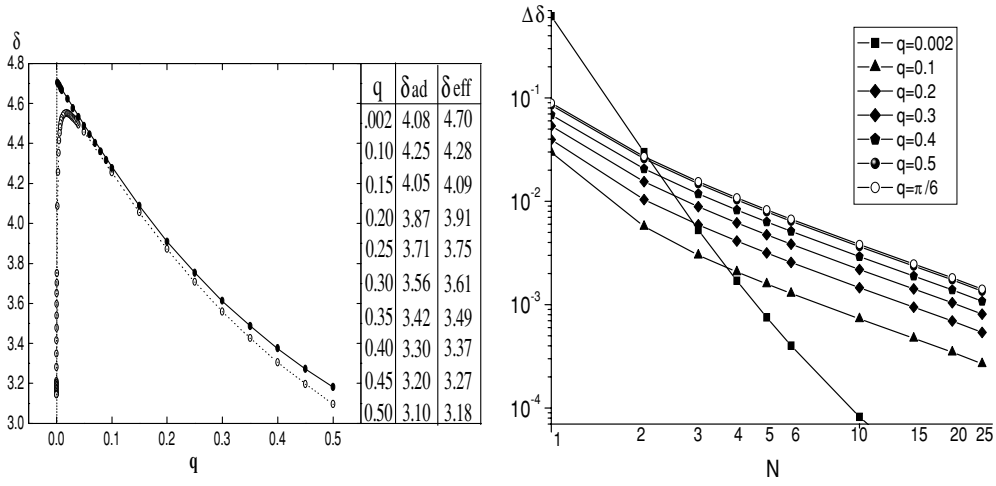

q	δad	δeff
.002	4.08	4.70
0.10	4.25	4.28
0.15	4.05	4.09
0.20	3.87	3.91
0.25	3.71	3.75
0.30	3.56	3.61
0.35	3.42	3.49
0.40	3.30	3.37
0.45	3.20	3.27
0.50	3.10	3.18

Figure 4. Elastic scattering phase shift δ as the function of the relative momentum q of the incident particle and the pair below the three-body-breakup threshold: (solid curve) exact analytical solution δ^{exact}; (dotted curve with open circles) results in the adiabatic approximation ($N = 1$), δ^{ad}; and (closed circles) results in the effective adiabatic approximation, δ^{eff} (left panel). The differences $\Delta\delta = \delta^{\text{exact}} - \delta^h$ of exact δ^{exact} and numerical δ^h results for the phase shift versus the number N of the radial equations at several relative momentum values belonging to the range $0 < q \leqslant \pi/6$ (right panel).

Table 3. The differences $\Delta\delta = \delta^{\text{exact}} - \delta^h$ of the exact and the numerical results (in the double precision) for the phase shift, versus the number N of equations (34) and the momentum proportional to q—using the Hulthèn variational functional. The factor x in the brackets means 10^x.

	q						
N	0.002	0.100	0.200	0.300	0.400	0.500	$\pi/6$
1	6.180(−1)	2.972(−2)	3.946(−2)	5.353(−2)	6.857(−2)	8.513(−2)	8.930(−2)
2	2.991(−2)	5.716(−3)	1.038(−2)	1.548(−2)	2.064(−2)	2.583(−2)	2.706(−2)
3	5.277(−3)	3.011(−3)	5.920(−3)	8.869(−3)	1.182(−2)	1.478(−2)	1.548(−2)
4	1.704(−3)	2.074(−3)	4.128(−3)	6.188(−3)	8.250(−3)	1.031(−2)	1.080(−2)
5	7.539(−4)	1.587(−3)	3.165(−3)	4.746(−3)	6.329(−3)	7.912(−3)	8.286(−3)
6	4.019(−4)	1.285(−3)	2.566(−3)	3.848(−3)	5.131(−3)	6.414(−3)	6.717(−3)
10	8.213(−5)	7.299(−4)	1.459(−3)	2.188(−3)	2.917(−3)	3.647(−3)	3.819(−3)
15	2.848(−5)	4.729(−4)	9.462(−4)	1.419(−3)	1.892(−3)	2.365(−3)	2.477(−3)
20	1.493(−5)	3.470(−4)	6.954(−4)	1.044(−3)	1.391(−3)	1.739(−3)	1.821(−3)
25	7.743(−6)	2.680(−4)	5.391(−4)	8.105(−4)	1.080(−3)	1.349(−3)	1.412(−3)

theoretical study [20]. In figure 5 we show an image of the half-bound-state function Ψ_{hb} at $q = 0$.

In the elastic scattering problem, we calculate the phase shift δ^h at $q\rho_m = 300$ and use 1500 fourth-order finite elements. The finite element grid consists of 6001 nodes. In table 3 we show the differences $\Delta\delta = \delta^{\text{exact}} - \delta^h$, calculated with an iteration scheme (38) based on the Hulthèn variational functional (39). One can see in the right panel of figure 4 that the KM converges monotonically to the exact values δ^{exact} at a rate of order $1/N$. Figure 5 also displays an image of the scattering wavefunction Ψ_0^s at $q = \pi/6$. The scattering length

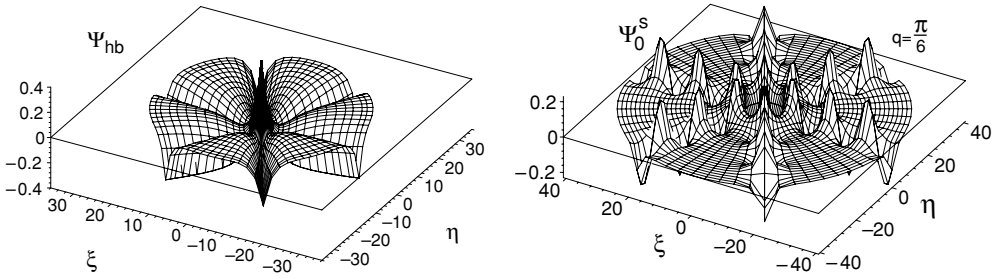

Figure 5. The half-bound state wavefunction Ψ_{hb} at $q = 0$, i.e. at the two-body threshold energy $2E_{hb} \approx -\pi^2/36$, for the attractive pair potentials (left panel). The scattering wavefunction Ψ_0^s at $q = \pi/6$, i.e. at the three-body threshold energy $2E = k^2 = 0$, for the attractive pair potentials (right panel).

Table 4. The differences $\Delta\delta = \delta^{\text{exact}} - \delta^h$ of the exact and the numerical results (in the double precision) for the phase shift, versus the number N of sums (40) and the momentum proportional to q—using the Hulthèn variational functional. The factor x in the brackets means 10^x.

	q						
N	0.002	0.100	0.200	0.300	0.400	0.500	$\pi/6$
1	6.180(−1)	2.972(−2)	3.946(−2)	5.353(−2)	6.857(−2)	8.513(−2)	8.930(−2)
2	2.928(−2)	5.331(−3)	9.679(−3)	1.430(−2)	1.903(−2)	2.464(−2)	2.616(−2)
3	3.954(−3)	2.557(−3)	5.104(−3)	7.548(−3)	1.006(−2)	1.345(−2)	1.445(−2)
4	3.186(−4)	1.607(−3)	3.293(−3)	4.842(−3)	6.458(−3)	8.960(−3)	9.747(−3)
5	−6.422(−4)	1.117(−3)	2.324(−3)	3.393(−3)	4.528(−3)	6.548(−3)	7.222(−3)
6	−9.966(−4)	8.140(−4)	1.723(−3)	2.491(−3)	3.327(−3)	5.047(−3)	5.651(−3)
10	−1.317(−3)	2.573(−4)	6.136(−4)	8.291(−4)	1.111(−3)	2.280(−3)	2.753(−3)
15	−1.371(−3)	1.055(−6)	1.018(−4)	6.219(−5)	9.081(−5)	1.008(−3)	1.424(−3)
20	−1.384(−3)	−1.220(−4)	−1.441(−4)	−3.056(−4)	−3.961(−4)	4.078(−4)	7.973(−4)
25	−1.390(−3)	−1.944(−4)	−2.884(−4)	−5.205(−4)	−6.776(−4)	6.703(−5)	4.439(−4)

$a_0 = -a = -\lim_{q\to 0}(\tan(\delta)/q) = -669.1664$ was calculated for $N = 1$ (note that the exact value $a_0 = -\infty$ is obtained as a limiting value, when N is taken very much larger than 1). A comparison of calculated values of the phase shift versus q, for the adiabatic approximation, EAA and exact formula is shown in the left panel of figure 4. One can see that the difference of the adiabatic and exact results increases with increasing q but disappears for the EAA calculations. Indeed, in table 4 we show the differences $\Delta\delta = \delta^{\text{exact}} - \delta^h$, calculated with an iteration scheme (47) based on the Hulthèn variational functional (48) for an EAA (40). We show also the values of the difference, $\Delta\delta = \delta^{\text{exact}} - \delta^h$ versus the number, N, of the corresponding upper bounds ($\Delta\delta > 0$) and lower bounds ($\Delta\delta < 0$) compared to the exact phase shift δ^{exact} of the scattering state below the three-body threshold. The change of a sign of this difference, when passing from $N = 4$ to $N = 5$ at $q = 0.002$, and $N = 15$ to $N = 20$ from $q = 0.1$ till $q = 0.4$, provides the lower bounds of phase shift of such scattering states, respectively. Thus, we have shown that the adiabatic approximation ($N = 1$) yields upper estimations for the scattering states above the pair threshold while EAA yields lower ones starting from $N > N_0(q)$, where the critical number $N_0(q)$ is increasing with increasing value of momentum q. In a vicinity below the three-body threshold a contribution of centrifugal term $q^2 W_{00}^{(N)} \rho^{-2}$ of equation (44) in asymptotic region predominates and is proportional to q in phase shift (49).

6. Conclusions

Stable numerical iteration schemes were developed to solve multi-dimensional differential equations, with high accuracy. New results were obtained for the solutions of these differential equations with long-range potentials. It has been shown that the numerical results that we obtained are in a good agreement with known exact results. Also, we saw that if we wish to use a very large number of orthogonal basis functions, we are forced to resort to quadruple precision arithmetic.

The benchmark problem, that we proposed, is a good tool to examine both the usefulness of various finite element method schemes (see, for example, [16, 18] and references therein) and, also, of the Kantorovich reduction [14]. The latter enables the reduction of the multi-dimensional Schrödinger equations to a set of second-order ordinary differential equations, in the context of the corresponding bound state and elastic scattering problems.

Our benchmark results may be expected to be very useful in the testing of new methods in the future. We feel that the effective Kantorovich approximations, with its canonical transformations, is the key to the development of substantially improved ways of obtaining accurate solutions to three-body scattering with a few open channels.

Acknowledgments

The authors thank Drs A G Abrashkevich and D V Pavlov for a long-time collaboration and Professors Yu N Demkov, V L Derbov and Drs K A Kouzakov, V V Pupyshev for useful discussions. AAT acknowledges partial support from CONACYT, project 41072-F. MSK and VAK acknowledge financial support from a grant of the President of the Bulgarian State Agency for Atomic Regulation 2004, the Bulgarian Fund for Scientific Investigations under grant I-1402/2004 and the theme 09-6-1060-2005/2007 'Mathematical support of experimental and theoretical studies conducted by JINR'. OC, AAG and SIV acknowledge partial support from the Russian Foundation for Basic Research under grant no. 03-02-16263.

Appendix A. Limiting and asymptotic behaviours of the matrix elements: the attractive case

As $\rho \to 0$ the potential curves $\epsilon_j(\rho)$ and the surface functions $B_j(\rho;\theta)$ take the form

$$\epsilon_0^{(\mathrm{sm})}(\rho) \to -\frac{1}{\rho}\left(1+\frac{\pi^2}{108}\rho+\frac{\pi^4}{14\,580}\rho^2\right), \qquad B_0^{(\mathrm{sm})}(\rho;\theta) \to \sqrt{\frac{1}{2\pi}},$$
$$\epsilon_j^{(\mathrm{sm})}(\rho) \to \left(\frac{6j}{\rho}\right)^2, \qquad B_j^{(\mathrm{sm})}(\rho;\theta) \to \sqrt{\frac{1}{\pi}}\cos[6j\theta(n)].$$

When $\rho \to \infty$, for finite i and j, $\epsilon_j(\rho)$ and $B_j(\rho;\theta)$ become asymptotically

$$\epsilon_0^{(\mathrm{as})}(\rho) \to -\frac{\pi^2}{36}\left(1+4\exp\left(-\frac{\pi^2\rho}{18}\right)\right), \qquad B_0^{(\mathrm{as})}(\rho;\theta) \to \frac{\sqrt{\pi\rho}}{6}\exp\left(-\frac{\rho\pi|\tilde{\theta}(n)|}{6}\right),$$
$$\epsilon_j^{(\mathrm{as})}(\rho) \to \left(\frac{6j-3}{\rho}\right)^2, \qquad B_j^{(\mathrm{as})}(\rho;\theta) \to \sqrt{\frac{1}{\pi}}\cos[(6j-3)\theta(n)],$$

where $\tilde{\theta}(n) = \pi/6 - |\theta(n)| \geqslant 0$, $\theta(n) = \theta - \pi n/3 \in (-\pi/6, \pi/6)$, $n = 0$–5.

For small ρ, the matrix elements $Q_{ij}(\rho)$ and $H_{ij}(\rho)$ behave (uniformly in i, j) as:

$$Q_{0j}(\rho) = +\frac{(-1)^j\sqrt{2}}{j^2}\left[\frac{1}{36}+\frac{\rho}{j^2}\left(\frac{1}{864}+\frac{\pi^2 j^2}{3888}\right)\right]+O(\rho^2),$$

$$Q_{ij}(\rho) = -\frac{(-1)^{i+j}}{i^2-j^2}\left[\frac{1}{18}+\frac{\rho}{1296}\left(\frac{1}{i^2}+\frac{1}{j^2}\right)\right]+O(\rho^2),$$

$$H_{00}(\rho) = \frac{\pi^4}{58\,320}+\frac{\pi^6}{2204\,496}\rho+O(\rho^2),$$

$$H_{jj}(\rho) = \frac{1}{j^4}\left(-\frac{1}{1728}+\frac{\pi^2 j^2}{3888}\right)+\frac{\rho}{j^6}\left(-\frac{13}{93\,312}+\frac{\pi^2 j^2}{17\,496}\right)+O(\rho^2),$$

$$H_{0j}(\rho) = \frac{(-1)^j\sqrt{2}}{j^4}\left[\frac{21-2\pi^2 j^2}{7776}+\frac{\rho}{j^2}\left(\frac{17}{62\,208}+\frac{\pi^2 j^2}{139\,968}-\frac{7\pi^4 j^4}{131\,220}\right)\right]+O(\rho^2),$$

$$H_{ij}(\rho) = \frac{(-1)^{(i+j)}}{(i^2-j^2)^2}\left[\frac{5}{648}-\frac{i^4+j^4}{1296 i^2 j^2}\right.$$
$$\left.+\rho\left(-\frac{\pi^2}{11\,664}+\frac{i^2+j^2}{3456 i^2 j^2}-\frac{11(i^6+j^6)}{93\,312 i^4 j^4}+\frac{\pi^2(i^4+j^4)}{23\,328 i^2 j^2}\right)\right]+O(\rho^2)$$

and for large values of ρ and finite values of the indices i and j $(i/\rho \ll 1 j/\rho \ll 1)$:

$$Q_{0j}(\rho) = +\frac{216(-1)^j(2j-1)}{\pi^2\rho^2\sqrt{\rho}}+\frac{11\,664(-1)^j(2j-1)}{\pi^4\rho^3\sqrt{\rho}}+O(\rho^{-9/2}),$$

$$Q_{ij}(\rho) = -\frac{18(-1)^{(i+j)}(2j-1)(2i-1)}{\pi^2(i-j)(i+j-1)}\left[\frac{1}{\rho^2}+\frac{36}{\pi^2\rho^3}\right.$$
$$\left.-\frac{162}{\pi^2\rho^4}\left(\frac{8}{\pi^2}-(2j-1)^2-(2i-1)^2\right)\right]+O(\rho^{-5}), \qquad \text{(A.1)}$$

$$H_{00}(\rho) = \frac{1}{4\rho^2}+\exp\left(-\frac{\pi^2\rho}{18}\right)\left(-\frac{\pi^2}{18\rho}-\frac{\pi^4}{324}+\frac{\pi^6}{17\,496}\rho\right)+O\left(\exp\left(-\frac{\pi^2\rho}{9}\right)\right),$$

$$H_{jj}(\rho) = \frac{108}{\pi^4\rho^4}(3+\pi^2(2j-1)^2)+O(\rho^{-5}),$$

$$H_{0j}(\rho) = \frac{108(-1)^j(2j-1)}{\pi^2\rho^3\sqrt{\rho}}+O(\rho^{-9/2}),$$

$$H_{ij}(\rho) = \frac{(-1)^{(i+j)}(2i-1)(2j-1)}{(i-j)^2(i+j-1)^2}\frac{324}{\pi^4\rho^4}((2j-1)^2+(2i-1)^2)+O(\rho^{-5}).$$

We now show how to obtain a further set of asymptotic results. We start by outlining a systematic method yielding the roots $y_j(\rho)$ of equation (15),

$$y_j(\rho)\tan(\pi y_j(\rho)) = x, \qquad j-\tfrac{1}{2} < y_j(\rho) < j, \quad j=1,2,\ldots, \qquad \text{(A.2)}$$

at $x \equiv c\pi\rho/36$, $c=-1$ and we present the roots $y_j(\rho)$ of equation (A.2) in the form

$$y_j(\rho) = j+z_j(\rho), \qquad -\tfrac{1}{2} < z_j(\rho) < 0.$$

In this notation (A.2) becomes

$$(j+z_j(\rho))\tan(\pi j+\pi z_j(\rho)) = x,$$

or

$$\pi z_j(\rho) = \arctan\left(\frac{x}{j+z_j(\rho)}\right) = \operatorname{arccot}\left(\frac{j}{x}+\frac{z_j(\rho)}{x}\right). \qquad \text{(A.3)}$$

For $|x| \gg 1$, we can expand the right-hand side of this equation in a series in the small parameter $z_j(\rho)/x = \varepsilon$, $|\varepsilon| \ll 1$, and find the leading approximation $z_j^{(0)}(\rho)$ to $z_j(\rho)$. To

calculate $z_j(\rho)$ to the required accuracy, we will write it in the form of a series with respect to a formal parameter λ

$$z_j(\rho) = z_j(\rho, \lambda) = z_j^{(0)}(\rho) + \sum_{n=1} \lambda^n z_j^{(n)}(\rho). \tag{A.4}$$

The λ will be put to 1 in the final results. Introducing the scaled variables $X = x\lambda$, $J = j\lambda$, we rewrite equation (A.3) as

$$\pi z_j(\rho) = \operatorname{arccot}\left(\frac{J}{X} + \lambda \frac{z_j(\rho)}{X}\right). \tag{A.5}$$

Substituting (A.4) into (A.5), we expand the right-hand side of equation (A.5) in a Taylor series with respect to the formal parameter λ. We obtain a recurrent set of algebraic equations for the unknown coefficients $z_j^{(n)}(\rho)$. We find the result:

$$z_j(\rho) = -\frac{\tilde{a}_j}{\pi} - \lambda \frac{\tilde{a}_j X}{\pi^2(X^2 + J^2)} - \lambda^2 \frac{\tilde{a}_j X(X + J\tilde{a}_j)}{\pi^3(X^2 + J^2)^2} + \lambda^3 \frac{\tilde{a}_j X\left(-9XJ\tilde{a}_j + X^2\left(\tilde{a}_j^2 - 3\right) - 3J^2\tilde{a}_j^2\right)}{3\pi^4(X^2 + j^2)^3} + O(\lambda^4),$$

where $\tilde{a}_i = \arctan(|x|/i)$ and $\tilde{a}_j = \arctan(|x|/j)$. For $|x| \gg 1$ one then has asymptotic expressions, uniform with respect to i and j, for the potential curves, surface functions and matrix elements. Letting $I = \lambda i$, $J = \lambda j$, $X = \lambda|x|$, we obtain:

$$\epsilon_i = \frac{\pi^2 i^2}{36|x|^2}\left(1 - \frac{2\tilde{a}_i}{i}(1 + o(1))\right) = \left(\frac{6i}{\rho}\right)^2 - \frac{72i\tilde{a}_i}{\pi\rho^2} + \cdots,$$

$$B_i = \frac{1}{\pi^{1/2}}\left[\cos(6i\theta(n)) + \frac{6\tilde{a}_i\theta}{\pi}\sin(6i\theta(n))\right](1 + o(1)),$$

$$Q_{0i} = \lambda^{3/2}\frac{(-1)^i\pi^{1/2}IX^{1/2}}{18(X^2 + I^2)^{3/2}} - \lambda^{5/2}\frac{(-1)^i X^{1/2}(2X^2\tilde{a}_i - XI - 4I^2\tilde{a}_i)}{36\pi^{1/2}(X^2 + I^2)^{5/2}} - \lambda^{7/2}\frac{(-1)^i X^{1/2}\left(12X^3\tilde{a}_i + 3X^2I\left(12\tilde{a}_i^2 - 1\right) - 32XI^2\tilde{a}_i - 24I^3\tilde{a}_i^2\right)}{144\pi^{3/2}(X^2 + I^2)^{7/2}} + O(\lambda^{9/2}),$$

$$H_{0i} = \lambda^{5/2}\frac{(-1)^i\pi^{3/2}I(X^2 - I^2)}{1296X^{1/2}(X^2 + I^2)^{5/2}} - \lambda^{7/2}\frac{(-1)^i\pi^{1/2}(2X^4\tilde{a}_i + 5X^3I - 14X^2I^2\tilde{a}_i - 9XI^3 + 4I^4\tilde{a}_i)}{2592X^{1/2}(X^2 + I^2)^{7/2}} + O(\lambda^{9/2}),$$

$$H_{ii} = -\lambda^3\frac{\pi I(X^2\tilde{a}_i - 3XI - I^2\tilde{a}_i)}{1944(X^2 + I^2)^3} + O(\lambda^4),$$

$$Q_{ij} = \lambda^2\frac{(-1)^{i+j}IJ}{18(J^2 - I^2)(X^2 + J^2)^{1/2}(X^2 + I^2)^{1/2}} - \lambda^3\left[\frac{(-1)^{i+j}2X^2(X^2 + I^2 + J^2)(I^2 + J^2)(J\tilde{a}_i - I\tilde{a}_j)}{36\pi(J^2 - I^2)^2(X^2 + J^2)^{3/2}(X^2 + I^2)^{3/2}} + \frac{(-1)^{i+j}XIJ(2X^2 + I^2 + J^2 + 2XI\tilde{a}_i + 2XJ\tilde{a}_j)}{36\pi(J^2 - I^2)(X^2 + J^2)^{3/2}(X^2 + I^2)^{3/2}} + \frac{(-1)^{i+j}4I^3J^3(I\tilde{a}_i - J\tilde{a}_j)}{36\pi(J^2 - I^2)^2(X^2 + J^2)^{3/2}(X^2 + I^2)^{3/2}}\right] + O(\lambda^4),$$

$$H_{ij} = \lambda^3\frac{XIJ\pi^2(-1)^{i+j}}{648(X^2 + I^2)^{3/2}(X^2 + J^2)^{3/2}} + O(\lambda^4).$$

Using, then, these asymptotic results, we find:

$$W^{(\infty)}(\rho) = -\frac{18}{\pi^2\rho^2} + O(\rho^{-4}) \approx -1.823\,78\rho^{-2},$$

$$\sum_{j=1}^{\infty} \Delta_{0j}^{-1} H_{0j}^2 = -\frac{9}{32\pi^2\rho^4} + O(\rho^{-5}) \approx -0.028\,49\rho^{-4},$$

$$-\sum_{j=1}^{\infty} \Delta_{0j}^{-1} (Q'_{0j})^2 = \frac{333}{32\pi^2\rho^4} + O(\rho^{-5}) \approx 1.054\,37\rho^{-4},$$

$$2\sum_{j=1}^{\infty} \Delta_{0j}^{-1} Q_{0j} H'_{0j} = \frac{9}{16\pi^2\rho^4} + O(\rho^{-5}) \approx 0.056\,99\rho^{-4},$$

$$-2\sum_{j=1}^{\infty} \Delta_{0j}^{-1} Q_{0j} Q''_{0j} = \frac{369}{16\pi^2\rho^4} + O(\rho^{-5}) \approx 2.336\,71\rho^{-4},$$

$$\sum_{j=1}^{\infty} \Delta_{0j}^{-2} H_{0j} Q_{0j} (\Sigma'_{0j} - \Delta'_{0j}) = O(\rho^{-5}),$$

$$\sum_{j=1}^{\infty} \Delta_{0j}^{-2} Q_{0j} Q'_{0j} (\Sigma'_{0j} + 3\Delta'_{0j}) = -\frac{27}{4\pi^2\rho^4} + O(\rho^{-5}) \approx -0.683\,91\rho^{-4},$$

$$\sum_{j=1}^{\infty} \Delta_{0j}^{-2} Q_{0j}^2 (\Sigma''_{0j} + \Delta''_{0j}) = O\left(\exp\left(-\frac{\pi^2\rho}{18}\right)\right),$$

$$\sum_{j=1}^{\infty} \Delta_{0j}^{-3} Q_{0j}^2 (\Sigma'_{0j} + \Delta'_{0j})(\Sigma'_{0j} - 2\Delta'_{0j}) = O\left(\exp\left(-\frac{\pi^2\rho}{18}\right)\right),$$

$$\delta U^{(\infty)}(\rho) = \frac{27}{\pi^2\rho^4} + O(\rho^{-6}) \approx 2.735\,67\rho^{-4}.$$

The calculated asymptotic values, $W^{(\infty)}(\rho)$ and $\delta U^{(\infty)}(\rho)$, confirm the numerical estimations (25) with a guaranteed accuracy of orders $O(\rho^{-4})$ and $O(\rho^{-6})$, respectively.

Appendix B. Asymptotic behaviour of the effective potentials

For the evaluation, as $\rho \to \infty$, of the matrix elements $Q_{0i}(\rho)$, $Q'_{0i}(\rho)$, $H_{00}(\rho)$ and $H_{0i}(\rho)$, involved in the definition of the effective mass and the non-adiabatic correction (24), we make the change of variables, $\eta = \rho\cos\theta$, for fixed ρ, in their defining expressions (13). If we put $6j/\rho = |p|$ and $6j\theta(n) = |p|\eta$, $j = 1, 2, \ldots$, then in each sector ($n = 0, \ldots, 5$) of the plane, $|\eta/\rho|$ will be $\ll 1$, and the basis $\{B_0(\rho;\theta), B_j(\rho;\theta)\}$ will correspond to the following set of asymptotic functions $\{\phi_0(\eta), \phi_p(\eta)\}$:

$$B_0(\rho;\theta) \to \sqrt{\rho}\phi_0(\eta), \qquad B_j(\rho;\theta) \to \frac{\phi_p(\eta)}{\cos(\delta(p))}. \tag{B.1}$$

Here $\delta(p) = -\arctan|p|/\bar{\kappa} + \pi/2$ is a phase shift, and the functions have the form

$$\phi_0(\eta) = \sqrt{\bar{\kappa}}\exp(-\bar{\kappa}|\eta|), \qquad \phi_p(\eta) = \sqrt{\frac{1}{\pi}}(\cos(p|\eta| + \delta(p)).$$

These functions are eigenfunctions of the corresponding eigenvalue problem

$$\begin{aligned} h^{(0)}\phi_0(\eta) &= \epsilon_0^{(0)}\phi_0(\eta), \qquad & \epsilon_0^{(0)} &= -\bar{\kappa}^2, \\ h^{(0)}\phi_p(\eta) &= \epsilon_p^{(0)}\phi_p(\eta), \qquad & \epsilon_p^{(0)} &= p^2, \end{aligned} \tag{B.2}$$

of the pair Hamiltonian, in one of the chosen pair channels (for $|\eta/\rho| \ll 1$):

$$h^{(0)} = -\frac{\partial^2}{\partial\eta^2} - 2\bar{\kappa}\delta(|\eta|).$$

They satisfy the following orthogonality and completeness relations:

$$\begin{aligned} \langle 0|0\rangle &= \int_{-\infty}^{+\infty} \phi_0^*(\eta)\phi_0(\eta)\,\mathrm{d}\eta = 1, \\ \langle 0|p\rangle &= \int_{-\infty}^{+\infty} \phi_0^*(\eta)\phi_{p'}(\eta)\,\mathrm{d}\eta = 0, \\ \langle p|p'\rangle &= \int_{-\infty}^{+\infty} \phi_p^*(\eta)\phi_{p'}(\eta)\,\mathrm{d}\eta = \delta(p-p'), \\ |\phi_0\rangle\langle\phi_0| &+ \int_0^{\infty} \mathrm{d}p|\phi_p\rangle\langle\phi_p| = 1. \end{aligned} \tag{B.3}$$

In this representation[6], the asymptotic Hamiltonian, corresponding to equations (10) in the chosen pair channel, takes the form

$$h(\eta,\rho) = h^{(0)} + \frac{1}{4\rho^2} - \frac{\hat{K}^{(0)}}{\rho^2}, \qquad \hat{K}^{(0)} = -\eta^2\frac{\partial^2}{\partial\eta^2} - \eta\frac{\partial}{\partial\eta} + \frac{1}{4}, \tag{B.4}$$

and expressions for the matrix elements $Q_{0j}(\rho) = -Q_{j0}(\rho)$, $K_{0j}(\rho) = H_{0j}(\rho) + Q'_{0j}(\rho)$, $H_{0j}(\rho) = H_{j0}(\rho)$ and $K_{00}(\rho) = H_{00}(\rho)$ read:

$$\begin{aligned} Q_{0p}(\rho) &= Q_{0p}^{(0)}\rho^{-1} + O(\rho^{-5/2}), \qquad & Q_{0p}^{(0)} &= \int_{-\infty}^{+\infty} \mathrm{d}\eta\phi_0^*(\eta)\hat{Q}^{(0)}\phi_p(\eta), \\ K_{0p}(\rho) &= H_{0p}(\rho) + \frac{\partial Q_{0p}(\rho)}{\partial\rho}, \qquad & K_{0p}(\rho) - K_{p0}(\rho) &= 2\frac{\partial Q_{0p}(\rho)}{\partial\rho}, \\ K_{0p} &= K_{0p}^{(0)}\rho^{-2} + O(\rho^{-7/2}), \qquad & K_{0p}^{(0)} &= \int_{-\infty}^{+\infty} \mathrm{d}\eta\phi_0^*(\eta)\hat{K}^{(0)}\phi_p(\eta) = H_{0p}^{(0)} - Q_{0p}^{(0)}, \\ H_{0p}(\rho) &= H_{0p}^{(0)}\rho^{-2} + O(\rho^{-5}), \qquad & H_{0p}^{(0)} &= \int_{-\infty}^{+\infty} \mathrm{d}\eta\phi_0^*(\eta)\hat{H}^{(0)}\phi_p(\eta), \end{aligned}$$

where

$$\phi_0^*(\eta)\hat{H}^{(0)}\phi_p(\eta) = \left(-\frac{1}{4}\phi_0^*(\eta)\phi_p(\eta) + \eta^2\frac{\partial\phi_0^*(\eta)}{\partial\eta}\frac{\partial\phi_p(\eta)}{\partial\eta}\right), \qquad Q^{(0)} = -\left(\frac{1}{2} + \eta\frac{\partial}{\partial\eta}\right).$$

For the matrix elements $Q_{0p}^{(0)}$, between the discrete and continuous eigenfunctions of the pair-channel Hamiltonian $h^{(0)}$ of equation (B.2), we obtain

$$Q_{0p}^{(0)} = -\tfrac{1}{4}\langle\phi_0[\eta^2, h^{(0)}]\phi_p\rangle = \tfrac{1}{4}\big(\epsilon_0^{(0)} - \epsilon_p^{(0)}\big)\langle\phi_0|\eta^2|\phi_p\rangle. \tag{B.5}$$

[6] Note that the asymptotic conditions correspond to a number $j > \pi\rho/36 + 1/2 = |x| + 1/2$ of the compact adiabatic basis.

Accordingly, we find

$$\begin{aligned}
&\langle 0|\eta^2|0\rangle = \frac{1}{2\bar\kappa^2}, \quad \langle 0|\eta^2|p\rangle = \sqrt{\frac{\bar\kappa}{\pi}}\frac{8\bar\kappa p}{(\bar\kappa^2+p^2)^{5/2}}, \quad H_{00}^{(0)} = \frac{1}{4},\\
&Q_{0p}^{(0)} = -\int_{-\infty}^{\infty} \mathrm{d}\eta\eta\phi_0(\eta)\frac{\partial}{\partial\eta}\phi_p(\eta) = -\sqrt{\frac{\bar\kappa}{\pi}}\frac{2\bar\kappa p}{(\bar\kappa^2+p^2)^{(3/2)}},\\
&H_{0p}^{(0)} = \int_{-\infty}^{\infty} \mathrm{d}\eta\eta^2\left(\frac{\partial}{\partial\eta}\phi_0(\eta)\right)\left(\frac{\partial}{\partial\eta}\phi_p(\eta)\right) = \sqrt{\frac{\bar\kappa}{\pi}}\frac{4\bar\kappa p(p^2-\bar\kappa^2)}{(\bar\kappa^2+p^2)^{(5/2)}}.
\end{aligned} \tag{B.6}$$

Using these results, we can evaluate the following sum rules:

$$\begin{aligned}
&4\int_0^{\infty}\mathrm{d}p\frac{Q_{0p}^{(0)}Q_{p0}^{(0)}}{\epsilon_0^{(0)}-\epsilon_p^{(0)}} = -\langle 0|\eta^2\hat{Q}^{(0)}|0\rangle = \langle 0|\eta^2|0\rangle = \frac{1}{2\bar\kappa^2},\\
&\int_0^{\infty}\mathrm{d}p\frac{H_{0p}^{(0)}H_{p0}^{(0)}}{\epsilon_0^{(0)}-\epsilon_p^{(0)}} = -\frac{1}{8\bar\kappa^2}, \qquad 4\int_0^{\infty}\mathrm{d}p\frac{Q_{0p}^{(0)}H_{p0}^{(0)}}{\epsilon_0^{(0)}-\epsilon_p^{(0)}} = -\frac{1}{4\bar\kappa^2}.
\end{aligned} \tag{B.7}$$

In the second order of conventional perturbation theory, with ρ^{-2} as a small parameter, and with $|j\rangle = |0\rangle$ for the ground state, we can write in one chosen pair channel (for $|\eta/\rho| \ll 1$):

$$h(\eta,\rho)\phi_j(\eta,\rho) = \epsilon_j(\rho)\phi_j(\eta,\rho), \tag{B.8}$$

$$\epsilon_j(\rho) = \epsilon_j^{(0)} + \rho^{-2}\epsilon_j^{(1)} + \rho^{-4}\epsilon_j^{(2)} + O(\rho^{-6}), \tag{B.9}$$

where

$$\begin{aligned}
&\epsilon_0^{(1)} = \frac{1}{4} - H_{00}^{(0)} = 0,\\
&\epsilon_0^{(2)} = \int_0^{\infty}\mathrm{d}p\frac{K_{0p}^{(0)}K_{p0}^{(0)}}{\epsilon_0^{(0)}-\epsilon_p^{(0)}} = \int_0^{\infty}\mathrm{d}p\frac{Q_{0p}^{(0)}Q_{p0}^{(0)}+H_{0p}^{(0)}H_{p0}^{(0)}}{\epsilon_0^{(0)}-\epsilon_p^{(0)}} = \frac{1}{8\bar\kappa^2}-\frac{1}{8\bar\kappa^2} = 0.
\end{aligned} \tag{B.10}$$

Using the above asymptotic forms for the potential curves and the matrix elements, and dropping the matrix elements between states of the continuous spectrum, we then have, using the representation of the pair channel $|i\rangle = |0\rangle$ in equation (B.8), the following approximation of the system (12) for the unknowns $\bar\chi^{\mathrm{as}} = \rho^{1/2}\chi$:

$$\begin{aligned}
&\left(\frac{\mathrm{d}^2}{\mathrm{d}\rho^2}+q^2\right)\bar\chi_{00}^{\mathrm{as}}(\rho,q) = \int_0^{\infty}\mathrm{d}p\left[\frac{H_{0p}^{(0)}-Q_{0p}^{(0)}}{\rho^2}+\frac{2Q_{0p}^{(0)}}{\rho}\frac{\mathrm{d}}{\mathrm{d}\rho}\right]\bar\chi_{p0}^{\mathrm{as}}(\rho,q),\\
&\left(\frac{\mathrm{d}^2}{\mathrm{d}\rho^2}-\epsilon_p^{(0)}+\epsilon_0^{(0)}+q^2\right)\bar\chi_{p0}^{\mathrm{as}}(\rho,q) = \left[\frac{H_{p0}^{(0)}-Q_{p0}^{(0)}}{\rho^2}+\frac{2Q_{p0}^{(0)}}{\rho}\frac{\mathrm{d}}{\mathrm{d}\rho}\right]\bar\chi_{00}^{\mathrm{as}}(\rho,q),
\end{aligned} \tag{B.11}$$

where $q^2 = \epsilon = 2E - \epsilon_0^{(0)}$—is twice the relative energy counted from the pair threshold $\epsilon_0^{(0)} = -\bar\kappa^2$.

Appendix C. Canonical asymptotic transformation

To find asymptotic solutions $\bar\chi^{\mathrm{as}}(\rho)$ of equations (B.11), in second order of an operator perturbation theory, we formally apply a canonical transformation, $T = \exp(\imath S^{(0)})$, to obtain a new representation where $\bar\chi^{\mathrm{new}}(\rho) = T\bar\chi^{\mathrm{as}}(\rho)$:

$$\begin{aligned}
&\bar\chi_{j0}^{\mathrm{as}} = T_{j0}^{-1}\bar\chi_{00}^{\mathrm{new}}, \qquad \bar\chi_{00}^{\mathrm{new}} = \sum_j T_{0j}\bar\chi_{j0}^{\mathrm{as}},\\
&\langle 0|T|0\rangle = \langle 0|T^{-1}|0\rangle = 1 = \langle 0|0\rangle.
\end{aligned} \tag{C.1}$$

This leads to a projection of the above system of equations onto the pair channel $|0\rangle$

$$\sum_{ij} T_{0i}(H^{\text{old}} - q^2)_{ij}\bar{\chi}^{\text{as}}_{j0} = \sum_{ij} T_{0i}(H^{\text{old}} - q^2)_{ij}T^{-1}_{j0}\bar{\chi}^{\text{new}}_{00}$$
$$= \left(H^{\text{new}}_{00} - q^2\right)\bar{\chi}^{\text{new}}_{00} = 0, \tag{C.2}$$

if the non-diagonal matrix elements of generator $S^{(0)}$ are defined by

$$\imath S^{(0)}_{0p} = \frac{1}{\left(\epsilon^{(0)}_0 - \epsilon^{(0)}_p\right)}\left(\frac{H^{(0)}_{0p} - Q^{(0)}_{0p}}{\rho^2} + \frac{2Q^{(0)}_{0p}}{\rho}\frac{\mathrm{d}}{\mathrm{d}\rho}\right), \tag{C.3}$$

which cancels the right-hand side of equation (B.11). Restricting the expansion of the exponential to second order, i.e., expressing $\exp(\imath S^{(0)}) \approx 1 + \imath S^{(0)} + (\imath S^{(0)})^2/2$, we obtain a unique pair channel equation, with an effective mass and potential for the state $|0\rangle$, in the new representation $\bar{\chi}^{\text{eff}} \equiv \bar{\chi}^{\text{new}}$:

$$\left(-\frac{\mathrm{d}}{\mathrm{d}\rho}\left(1 + \frac{W^{(0)}_{00}}{\rho^2}\right)\frac{\mathrm{d}}{\mathrm{d}\rho} + \frac{\delta U^{(0)}_{00}}{\rho^4} - q^2\right)\bar{\chi}^{\text{new}}_{00}(\rho) = 0. \tag{C.4}$$

Using sum rules (B.7), we explicitly calculate the asymptotic values of corrections for an effective mass

$$W^{(0)}_{00} = -4\int_0^\infty \mathrm{d}p \frac{Q^{(0)}_{0p}Q^{(0)}_{p0}}{\epsilon^{(0)}_0 - \epsilon^{(0)}_p} = -\langle 0|\eta^2|0\rangle = -\frac{1}{2\bar{\kappa}^2} \tag{C.5}$$

and for an effective potential

$$\delta U^{(0)}_{00} = \int_0^\infty \mathrm{d}p \frac{\left(H^{(0)}_{0p}\right)^2 - \left(Q^{(0)}_{0p}\right)^2 - 4Q^{(0)}_{0p}H^{(0)}_{0p} - 4\left(Q^{(0)}_{0p}\right)^2}{\left(\epsilon^{(0)}_0 - \epsilon^{(0)}_p\right)}$$
$$\equiv \int_0^\infty \mathrm{d}p \frac{V^{(1)}_{0p}}{\Delta^{(0)}_{0p}} = \left(-\frac{1}{8\bar{\kappa}^2} + \frac{1}{8\bar{\kappa}^2} + \frac{1}{4\bar{\kappa}^2} + \frac{1}{2\bar{\kappa}^2}\right) \equiv \frac{3}{4\bar{\kappa}^2}. \tag{C.6}$$

For large ρ, to an accuracy of order $O(\rho^{-4})$, equation (C.4) reads

$$\left[\frac{\mathrm{d}^2}{\mathrm{d}\rho^2} - \frac{2W^{(0)}_{00}}{\rho^3}\frac{\mathrm{d}}{\mathrm{d}\rho} + q^2\left(1 - \frac{W^{(0)}_{00}}{\rho^2}\right) - \frac{\delta U^{(0)}_{00}}{\rho^4}\right]\bar{\chi}^{\text{new}}_{00}(\rho) = 0. \tag{C.7}$$

For $q\langle 0|\eta^2|0\rangle/(2\rho) \ll 1$, the continuous spectrum solutions of equation (C.7) can be put into the form

$$\bar{\chi}^{\text{new}}_{00}(\rho) \sim \sin\left[q\rho\left(1 - \frac{\langle 0|\eta^2|0\rangle}{2\rho^2}\right) + \delta\right]$$
$$\approx \sin(q\rho + \delta) - q\frac{\langle 0|\eta^2|0\rangle}{2\rho}\cos(q\rho + \delta), \tag{C.8}$$

where $\delta \equiv \delta(q)$ is the phase shift of the elastic scattering in the open pair channel $|0\rangle$, below the main three-body threshold, $E = 0$. The solutions $\bar{\chi}_p(\rho)$ of the system (B.11) are connected with the solution $\bar{\chi}^{\text{new}}_{00}(\rho)$ of the effective equation (C.7) by the inverse asymptotic transformation (C.1), which reveals a weak asymptotic coupling of the closed channels

$$\bar{\chi}^{\text{as}}_{j0}(\rho) = T^{-1}_{j0}\bar{\chi}^{\text{new}}_{00}(\rho) \sim \exp\left[-\frac{\langle j|\eta^2|0\rangle(1 - \delta_{j0})}{2\rho}\frac{\mathrm{d}}{\mathrm{d}\rho}\right]\bar{\chi}^{\text{new}}_{00}(\rho). \tag{C.9}$$

Using (C.8) into the above, we obtain asymptotic solutions for equations (B.11),

$$\begin{aligned}\bar{\chi}^{\rm as}_{00}(\rho) &= \bar{\chi}^{\rm new}_{00}(\rho),\\ \bar{\chi}^{\rm as}_{j0}(\rho) &= T^{-1}_{j0}\bar{\chi}^{\rm new}_{00}(\rho) \sim -\frac{\langle j|\eta^2|0\rangle(1-\delta_{j0})}{2\rho} q\cos(q\rho+\delta).\end{aligned} \tag{C.10}$$

The partial component F in the two-body channel $|0\rangle$

$$F_0 = \left(|\phi_0\rangle\langle\phi_0|\phi_0\rangle + \int_0^\infty {\rm d}p|\phi_p\rangle\langle\phi_p|T^{-1}|\phi_0\rangle\right)\bar{\chi}^{\rm new}_{00}(\rho), \tag{C.11}$$

subject to the completeness condition (B.3), is defined by the relation

$$F_0 \sim \phi_0(\eta)\left[\sin(q\rho+\delta) - q\frac{\eta^2}{2\rho}\cos(q\rho+\delta)\right]. \tag{C.12}$$

For $q\eta^2/(2\rho) \ll 1$, we have, with an accuracy of order $O(\rho^{-1})$, a true separable representation in terms of the Jacobi coordinates (ξ, η)

$$F_0(\rho,\eta) \sim \phi_0(\eta)\sin\left[q\left(\rho - \frac{\eta^2}{2\rho}\right) + \delta(q)\right] \to \phi_0(\eta)\sin(q|\xi| + \delta(q)) \sim \phi_0(\eta)\bar{\chi}^{(0)}_{00}(\xi). \tag{C.13}$$

It is evident that, with increasing q, the role of the nonadiabatic coupling grows. In general, the discrepancy between $\xi \sim \rho(1-\eta^2/(2\rho^2))$ and $\rho = \sqrt{\xi^2+\eta^2}$, which leads to the weak asymptotic coupling in equation (C.9), can be neglected only in the adiabatic limit $q \to 0$. So, if we omit the nonadiabatic term in equation (C.7) and take the adiabatic behaviour

$$\bar{\chi}_{\rm ad} \sim \sin(q\rho + \delta^{\rm ad}(q)), \tag{C.14}$$

we then find the obvious difference between the true and the adiabatic phase shifts δ and $\delta^{\rm ad}$,

$$\delta(q) = \delta^{\rm ad}(q) + q\frac{\langle 0|\eta^2|0\rangle}{2\rho}. \tag{C.15}$$

Thus, we have found not only an effective approximation (C.4)–(C.7) for the system (B.11) of the adiabatic equations, but also a way to find the asymptotic behaviour of their solutions.

References

[1] Mott H F and Massey H S 1965 *Theory of Atomic Collisions* (London/New York: Oxford University Press)
[2] Faifman M P, Ponomarev L I and Vinitsky S I 1976 *J. Phys. B: At. Mol. Phys.* **9** 2255–68
Ponomarev L I and Vinitsky S I 1979 *J. Phys. B: At. Mol. Phys.* **12** 567–84
[3] Ponomarev L I, Vinitsky S I and Vukajlovich F R 1980 *J. Phys. B: At. Mol. Phys.* **13** 847–67
[4] Vinitsky S I and Ponomarev L I 1982 *Sov. J. Part. Nucl.* **13** 557–87
Bracci L and Fiorentini G 1982 *Phys. Rep.* **86** 169–216
Bracci L, Chiccoli C, Pasini P, Fiorentini G, Melezhik V S and Wozniak J 1990 *Nuovo Cimento* **105** 459–69
Korobov V I 1994 *J. Phys. B: At. Mol. Opt. Phys.* **27** 733–45
Chuluunbaatar O, Joulakian B B, Tsookhuu Kh and Vinitsky S I 2004 *J. Phys. B: At. Mol. Opt. Phys.* **37** 2607–16
[5] Fano U and Rau A R P 1986 *Atomic Collisions and Spectra* (Florida: Academic)
[6] Maček J 1968 *J. Phys. B: At. Mol. Phys.* **1** 831–43
Fano U 1983 *Rep. Prog. Phys.* **46** 97–165
Lin C D 1986 *Adv. Atom. Mol. Phys.* **22** 77–142
Lin C D 1995 *Phys. Rep.* **257** 1–83
[7] Ballot J L, Fabre de la Ripelle M and Levinger M 1982 *Phys. Rev.* C **26** 2301–9
[8] Larsen S Y 1986 *Few-Body Methods* (Singapore: World Scientific) 467
[9] Kadomtsev M B and Vinitsky S I 1986 *J. Phys. B: At. Mol. Phys.* **19** L765–71
Kadomtsev M B and Vinitsky S I 1987 *J. Phys. B: At. Mol. Phys.* **20** 5723–36
Abrashkevich A G, Kaschiev M S, Puzynin I V and Vinitsky S I 1986 *Sov. J. Nucl. Phys.* **48** 602–701

Dubovik V M, Markovski B L, Suzko A A and Vinitsky S I 1989 *Phys. Lett.* A **142** 133–8
Abrashkevich A G, Abrashkevich D G, Puzynin I V and Vinitsky S I 1991 *J. Phys. B: At. Mol. Opt. Phys.* **24** 1615–38
Vinitsky S I, Markovski B L and Suzko A A 1992 *Yad. Fiz.* **55** 669–87
Vinitsky S I, Markovski B L and Suzko A A 1992 *Sov. J. Nucl. Phys.* **55** 371–80 (Engl. Transl.)
Bernabeu J, Suslov V M, Strizh T A and Vinitsky S I 1996 *Hyperfine Interact.* **101/102** 391–9
[10] Abrashkevich A G, Abrashkevich D G and Shapiro M 1995 *Comput. Phys. Commun.* **90** 311–39
Abrashkevich A G, Puzynin I V and Vinitsky S I 2000 *Comput. Phys. Commun.* **125** 259–81
[11] Pack R T and Parker G A 1987 *J. Chem. Phys.* **87** 3888–921
Kress J D, Parker G A, Pack R T, Archer B J and Cook W A 1989 *Comput. Phys. Commun.* **53** 91–108
Archer B J, Parker G A and Pack G A 1990 *Phys. Rev.* A **41** 1303–10
[12] Kantorovich L V and Krylov V I 1964 *Approximate Methods of Higher Analysis* (New York: Wiley)
[13] Abrashkevich A G, Kaschiev M S and Vinitsky S I 2000 *J. Comp. Phys.* **163** 328–48
[14] Dimova M G, Kaschiev M S and Vinitsky S I 2005 *J. Phys. B: At. Mol. Opt. Phys.* **38** 2337–52
[15] Duff M, Rabitz H, Askar A, Cakmak A and Ablowitz M 1980 *J. Chem. Phys.* **72** 1543–59
Flores J R, Clementi E and Sonnad V 1989 *J. Chem. Phys.* **91** 7030–8
Ackermann J, Erdmann B and Roitzsch R 1994 *J. Chem. Phys.* **101** 7643–50
Yu H and Bandrauk A D 1995 *J. Chem. Phys.* **102** 1257–65
Dudley T J, Pandey R R, Staffin P E, Hoffmann M R and Schatz G C 2001 *J. Chem. Phys.* **114** 6166–79
Soares Neto J J and Prudente F V 1994 *Theor. Chim. Acta* **89** 415–27
Prudente F V and Soares Neto J J 1999 *Chem. Phys. Lett.* **302** 43–8
[16] Jaquet R 1990 *Comput. Phys. Commun.* **58** 257–69
Guimarães M N and Prudente F V 2005 *J. Phys. B: At. Mol. Opt. Phys.* **38** 2811–25
[17] Hipes P G and Kuppermann A 1987 *Chem. Phys. Lett.* **133** 1–7
Linderberg J, Padkjær S B, Öhrn Y and Vessal B 1989 *J. Chem. Phys.* **90** 6254–65
Shertzer J and Botero J 1994 *Phys. Rev.* A **49** 3673–9
[18] Prudente F V and Soares Neto J J 1999 *Chem. Phys. Lett.* **309** 471–8
[19] Gibson W, Larsen S Y and Popiel J J 1987 *Phys. Rev.* A **35** 4919–29
[20] Amaya-Tapia A, Larsen S Y and Popiel J J 1997 *Few-Body Syst.* **23** 87–109
[21] Vinitsky S I, Larsen S Y, Pavlov D V and Proskurin D V 2001 *Phys. At. Nuclei* **64** 27–37
[22] Chuluunbaatar O, Gusev A A, Larsen S Y and Vinitsky S I 2002 *J. Phys. A: Math. Gen.* **35** L513–25
[23] Demkov Yu N 1963 *Variational Principles in the Theory of Collisions* (Oxford: Macmillan/Pergamon)
[24] Rayleigh Lord 1873, 1937 *Theory of Sound* vol 1, sec 88 (London: MacMillan)
Ritz W 1909 *J. Reine Angew. Math.* **135** 1–61
[25] Hulthèn L 1944 *Kungl. Fysio. Sällskapets Lund Förhand.* **14** 257–69
[26] Strang G and Fix G J 1973 *An Analysis of the Finite Element Method* (Englewood Cliffs, NJ: Prentice-Hall)
[27] Bathe K J 1982 *Finite Element Procedures in Engineering Analysis* (Englewood Cliffs, NJ: Prentice-Hall)
[28] Abrashkevich A G, Abrashkevich D G, Kaschiev M S and Puzynin I V 1995 *Comput. Phys. Commun.* **85** 40–64
Abrashkevich A G, Abrashkevich D G, Kaschiev M S, Puzynin I V and Vinitsky S I 1997 *Preprint* JINR E11-97-335